

Final Draft

Analysis of Performance of the Inner Harbor Navigation Canal (IHNC)

Executive Summary

Four breaches occurred on the IHNC (Inner Harbor Navigation Canal) during Hurricane Katrina, on the morning of August 29th. Two of the breaches occurred on the east bank between the Florida Avenue Bridge and the North Claiborne Avenue Bridge adjacent to the 9th Ward, and two on the west bank just north of the intersection of France Road and Florida Avenue (Figure 1). Three of the breaches involved failures of floodwalls on levees, and one involved failure of a levee.

All of the IHNC floodwalls and levees were overtopped on August 29th. The peak storm surge elevation in the IHNC was 14.2 ft¹ at 9:00 AM, about 1.7 ft above the tops of the floodwalls and levees. The reaches where the floodwalls and levees did not collapse have therefore survived water loading considerably higher than the design loading.

Water flowing over the I-walls when they were overtopped eroded trenches on the protected side of the walls as it cascaded onto the levee fill. Soil that was providing support for the walls eroded away, making the walls less stable.

Although it is clear that the walls were overtopped, and that their stability was compromised by the erosion that occurred, it is also clear that one of the east side breaches occurred before the wall was overtopped. Eyewitness reports indicate that the water level in the 9th Ward near Florida Avenue was rising as early as 5:00 AM, when the water level in the IHNC was still below the top of the floodwall. Stability analyses indicate that foundation instability would occur before overtopping at the north breach on the east side of the IHNC. This breach location is thus the likely source of the early flooding in the 9th Ward. Stability analyses indicate that the other three breach locations would not have failed before they were overtopped.

The soil immediately beneath the levees and floodwalls at all four breach locations included marsh, beneath which was clay, and beneath the clay, sand. Through most of their lengths, the critical circles passed through the marsh and clay. The critical circles did not extend to the sand layer beneath the clay.

Stability analyses of the north breach on the east side resulted in a computed factor of safety equal to 1.0 with a crack on the canal side of the wall and water in the IHNC at elevation 11.2 ft. This is about 1.0 ft higher than the average IHNC water level at the time flood water was observed in the 9th Ward. Considering that the effective water level could have been one foot higher due to wave effects, this result is consistent with the observed IHNC water level when flood water was first reported in the 9th Ward.

¹ All elevations refer to NAVD88(2004.65) datum.

It thus appears that the north breach occurred before overtopping, and that this breach was the source of the first influx of water into the 9th Ward.

Stability analyses of the south breach on the east side, and the north breach on the west side, resulted in computed factors of safety larger than 1.0 with the water level at the top of the wall and a crack behind the wall, indicating that the walls at those locations would have remained stable if none of the soil supporting the wall had been removed by erosion. Stability analysis of the south breach on the west side, where there was no I-wall, showed that the factor of safety there was also high, and the failure was due to overtopping erosion.

The lower computed factor of safety at the north breach on the east side is attributable to the fact that the ground elevation on the protected side is lower at that location, and as a result there was less soil on the protected side of the wall that was able to provide support for the wall.

The IPET strength model used for the north breach on the east bank, which is based on all of the data available in May 2006, agrees fairly closely with the design strengths reported in the GDM² under the center of the levee. Both the GDM and the IPET strength model assign lower strengths beneath the embankment toe and beyond than beneath the crest of the embankment, but the GDM strengths at this location are higher than the IPET strengths. The GDM strengths are thus reasonably consistent with the currently available data.

The design analyses were performed using the Method of Planes³, without a crack between the wall and the levee fill on the canal side of the wall. For the canal water level at 10.5 ft (the design water level), the factor of safety computed using the Method of Planes was 1.25. The minimum factor of safety calculated for the same conditions using Spencer's method⁴ was 1.45, indicating that the Method of Planes is conservative by about 14% in this case.

In summary, the failure that resulted in the north breach on the east side of the IHNC resulted from two differences between the stability analyses that were used as the basis for design and those described in this report: (1) the ground surface beyond the toe of the levee at the north breach location was lower than the landside ground surface in the design cross section, and (2) the design analyses did not consider the possibility of a crack forming behind the wall, allowing water to run into the gap and increase the load on the wall. The other three breaches on the IHNC were due to overtopping and erosion.

² Design Memorandum No. 3, General Design, Lake Pontchartrain, LA, and Vicinity, Chalmette Area Plan, U.S. Army Engineer District, New Orleans, October 1966.

³ A study of the Method of Planes, undertaken by IPET at the request of the New Orleans District Task Force Guardian, indicates that the Method of Planes gives lower factors of safety than more accurate methods of analysis, such as Spencer's method. The magnitude of the difference between the two varies from case to case.

⁴ Spencer, E. (1967) "A Method of Analysis of the Stability of Embankments Assuming Parallel Inter-Slice Forces," *Geotechnique*, Institution of Civil Engineers, Great Britain, Vol. 17, No. 1, March, pp. 11-26.

Observations and Possible Modes of Failure

As shown by the hydrograph in Figure 2, the water level in the IHNC rose from elevation 1.0 ft. at 12:00 AM on August 28th to 14.2 ft. at 9:00 AM on August 29th. The peak water level was 1.7 ft. above the tops of the floodwalls and levees which were at elevation 12.5 ft. The hydrograph in Figure 3 shows that the water level in the 9th Ward was rising at 5:00 AM on August 29th, when the water level in the IHNC was at elevation 10.2 ft., about 2.3 ft. below the tops of the floodwalls and levees. With ground surface elevations approximately -4.0 ft., water at elevation +2.0 ft. indicates that the water was 6.0 ft. deep in the 9th Ward at 5:00 AM on August 29th.

Initial observations after the hurricane revealed that overtopping had eroded at least one section of levee along the west bank and had eroded the soil adjacent to the wall on the protected side along the east and west bank. It appeared that water flowing over the floodwall scoured and eroded the levee on the protected side of the I-wall, exposing the supporting sheet piles and reducing the passive resistance (Figure 4). The erosion appeared to be so severe in the breach locations that the sheet piles may have lost all of their foundation support, resulting in failure (Figure 5). Perhaps the best evidence of this scour can be seen along the unbreached reaches of the east bank I-walls on the Inner Harbor Navigation Canal where U-shaped scour trenches could be found adjacent to the I-walls. As the scour increased, the I-wall may have moved laterally and leaned to the protected side, causing the scour trench to grow as the water began cascading farther down the slope until sufficient soil resistance was lost and the wall was carried landward.

Other possible modes of failure are sliding instability and piping and erosion from underseepage. Piping and erosion from underseepage is unlikely because the I-walls were founded in a clay levee fill, a marsh layer made up of organics, clay and silt, and a clay layer. Because of the thickness, the low permeabilities of these materials, and the relatively short duration of the storm, this failure mode was considered not likely and was eliminated as a possible mode of failure.

It is necessary to investigate the possibility of sliding instability to determine if the I-walls could breach as a result of shear through the foundation. The foundation conditions are similar to the 17th Street Canal. As shown in Figure 6, no significant wall movement was found in the wall sections adjacent the south breach. However, Figure 7 shows significant wall movement did occur in the wall sections adjacent to the north breach.

Stratigraphy

IHNC East Bank – Lower 9th Ward

The data available to assess the stratigraphy of the area includes borings from the General Design Memorandum (GDM), borings taken after the failure, and cone penetration tests taken after the failure. The locations of these borings and cone penetration tests are shown in Figure 8. Note that all borings taken after the failure were

at the levee toe. The GDM contains 10 borings on the levee centerline (2-U, 3, 4, 5, 6-U and 7 in the vicinity of the breach, and four at the levee toe (2-UT, 3T, 4T and 6UT). A centerline profile under the levee is represented in Figure 9 and is based on both pre-Katrina and post-Katrina borings. This section shows 60 to 70 ft of predominantly fine-grained Holocene (i.e., less than 10,000 years old) shallow water and terrestrial sediments overlying the Pleistocene surface (i.e., older than 10,000 years). Holocene sediments are separated into various depositional environments in Figure 9, based on soil texture, organic content, and other physical and engineering properties. Engineering properties of these layers are described in greater detail below.

The sections of the IHNC east bank where the north and south breaches occurred encompass Stations 54+00 to 56+00 and 22+00 to 31+00, respectively. These breaches occurred between Florida Avenue and North Claiborne Avenue. The strength evaluation focused primarily on these areas.

The GDM borings indicate the levee fill properties for the north and south breach areas are similar, consisting of compacted CL and CH materials. The average moist unit weight of the fill was estimated to be 109 pcf.

Beneath the fill is a marsh unit about 17 ft thick. The marsh layer is composed of organic material from the cypress swamp that occupied the area, together with silt and clay deposited in the marsh. Because the upper 8 to 9 ft of this unit has different material properties than the lower portion, it was divided into two layers, Marsh 1 and Marsh 2. Water contents and moist unit weights determined from samples of marsh material taken from the toe are shown in Figures 10 and 11, respectively. These figures clearly depict the differences in the marsh layers.

Water contents, unit weights and undrained shear strengths are shown in Table 1, and these properties for the Marsh 2 layer are shown in Table 2. These properties are based on samples from post-Katrina borings at the levee toe. The average moist unit weight of the Marsh 1 layer is about 105 pcf. Water contents of the Marsh 1 layer are as high as 80%. The average water content is approximately 49%. The average moist unit weight of the Marsh 2 layer is about 80 pcf. Water contents of the marsh 2 layer are as high as 442%. The average water content is approximately 175%. The marsh 1 layer is mostly CH material. The Marsh 2 layer is fibrous at the top, and more amorphous near the bottom, indicating more advanced decomposition of the older organic materials at depth.

Beneath the marsh layers is a layer of interdistributary clay with an average Liquid Limit of about 79% and an average Plastic Limit of 26%. Based on consolidation test results presented in the GDM, the clay is normally consolidated throughout its depth. The average moist unit weight of the clay is about 100 pcf, and the average water content is approximately 60%. Water content and unit weights are summarized in Table 3.

Beneath the clay is a layer of Beach Sand. This layer is not involved in the observed or calculated mechanisms of instability, and its strength is therefore of little importance in stability analyses, except as a more resistant layer beneath the clay.

The unit weights measured for individual laboratory test specimens and the values used in subsequent analyses are shown in Figure 11.

Table 1. Properties of Marsh 1 layer from post-Katrina borings at toe

Marsh 1 Layer					
Number of Samples = 16					
	Mean	Standard Deviation	COV	Max	Min
% w	49	17	0.342	80.2	21.9
Moist Unit Weight (pcf)	104	9	0.081	120.5	92.2
Su (psf)	550	214	0.389	3195	90.0

Table 2. Properties of Marsh 2 layer from post-Katrina borings at toe

Marsh 2 Layer					
Number of Samples = 12					
	Mean	Standard Deviation	COV	Max	Min
% w	175	96	0.549	441.6	90.9
Moist Unit Weight (pcf)	78.4	7	0.091	87.1	63.4
Su (psf)	195.3	116	0.595	336	64.6

Table 3. Properties of interdistributary clay from post-Katrina borings at toe

Interdistributary Clay					
Number of Samples = 45					
	Mean	Standard Deviation	COV	Max	Min
% w	60	12	0.208	77.2	25
Moist Unit Weight (pcf)	101.1	6	0.063	125	93.6

Shear Strength - IHNC – East Bank

The sources of shear strength data include borings from the General Design Memorandum (GDM), and borings, cone penetration tests, and vane shear tests performed as part of the failure investigation. From the available sources, two GDM borings, four cone penetration tests, and three vane shear tests provide information beneath the centerline of levee. From the GDM borings (2-U and 6-U), the results of 11 Q test envelopes and 26 unconfined compression tests were available. All laboratory tests were performed on specimens trimmed from 5-in diameter undisturbed tube samples.

Beneath the toe of the levee, the GDM contained the results of over 70 unconfined compression tests. In addition, about 100 unconfined compression tests have been conducted on test specimens obtained since Katrina. Tests were performed on 1.4-inch diameter specimens trimmed from 5-in.-diameter tube samples. Statistical analyses have been performed on the data from the post-Katrina tests to compute minimum, maximum, and average values of strength for the levee fill, the marsh layers, and the clay. The results of the statistical analyses are shown in Tables 1 through 3. Also, one cone penetration test with pore pressure measurements (CPTU) and one series of vane shear tests were performed near the area of the breaches after the failure.

Shown in Figure 12 are the available laboratory and vane shear test results for samples obtained beneath the crest of the levee, as well as values of undrained shear strength determined from CPTU-1 using Mayne's method⁵. Figure 13 presents the data available for undrained shear strength from the toe of the levee and areas beyond the toe. Plotted with these data are the results from CPTU-1T, which was performed at the toe of the levee.

Only a few strength tests for the levee fill are available from GDM borings in the breach area. The shear strength used for design ($s_u = 500$ psf) was assumed for the levee-fill strength in the IPET strength model. As can be seen in Figure 12, a value of $s_u = 500$ psf for the levee fill seems reasonable based on the results of the CPTU tests, vane shear tests, and laboratory tests. However, the strength of the levee is not much involved in the calculated mechanisms of instability and therefore has limited importance in the stability analyses.

The marsh material is stronger beneath the levee crest where it has been compressed under the weight of the levee, and weaker at the toe of the levee and beyond, where it has not been compressed so heavily. CPTU data, vane shear tests, and unconfined compression tests conducted on test specimens trimmed from 5-in. samples were used to measure the Marsh 1 layer strengths at the toe. The measured shear strengths from the unconfined compression tests in the Marsh 1 layer scatter very widely from about 90 psf to over 800 psf, as shown in Figures 12 and 13. The vane shear test results summarized in Table 4 were conducted under the levee; they indicate shear strengths (corrected for strain rate effects and plasticity) ranging from 490 psf to 820 psf. Values of $s_u = 650$ psf beneath the levee crest, and $s_u = 550$ psf beneath the levee toe appear to be reasonably representative of the measured strengths for Marsh 1 layer, and these values are shown by the solid lines on Figures 12 and 13.

Table 4. IHNC east bank - results of vane shear tests in Marsh 1 layer, beneath levee.

Vane Shear Tests	Elev. ft NAVD88	%w	PI	Corrected Peak Strength (psf)
IHNC-VST-3	-6.3	--	--	732
IHNC-VST-6	-5.8	73	56	489
IHNC-VST-6	-10.8	--	--	566
IHNC-VST-1	-3.3	--	--	818
Average				651

The shear strength characterization of the Marsh 2 layer was difficult because of large scatter in the data. Data obtained from post-Katrina toe borings taken between

⁵ Mayne, P. W. (2003). "Class 'A' Footing Response Prediction from Seismic Cone Tests," Proceedings, Deformation Characteristics of Geomaterials, Vol. 1, Lyon, France.

Florida Avenue and North Claiborne Avenue are presented in Table 2. Noting Figures 12 and 13, which include both pre-Katrina and post-Katrina strength results, the undrained shear strength of the Marsh 2 layer ranges from about 200 to 620 psf under the levee centerline, and from 90 to 500 psf beneath the levee toe. Values of $s_u = 300$ psf beneath the levee crest, and $s_u = 200$ psf beneath the levee toe appear to be reasonably representative of the measured values; these values are shown on Figures 12 and 13. These strengths are the same as were used in the GDM design analyses.

Interpretation of the undrained shear strength of the interdistributary clays was developed considering the results of all laboratory and field tests. The pore pressure results from the CPTU tests were questionable, and for this reason, less emphasis was placed on determining undrained shear strengths from the cone penetration test results. The CPTU tests did indicate that the clay deposit was normally consolidated, and that the undrained shear strength increased linearly with depth. Figure 12 shows the undrained shear strength with depth determined using Mayne's method⁶ for CPTU-1, which was conducted under the centerline of the levee. Figure 13 presents the results of CPTU-1T, which was conducted at the toe of the levee.

The straight line shown in Figure 12, representing the average undrained shear strength in the clay, has a slope of 8.6 psf per foot of depth. This rate of strength increase with depth appears to compare reasonably well to the laboratory strength test results.

The rate of increase of strength with depth is directly related to the s_u/p' ratio for the clay and its buoyant unit weight as follows:

$$\frac{s_u}{p'} = \frac{\text{rate of increase of } s_u \text{ with depth}}{\text{rate of increase of } p' \text{ with depth}} = \frac{\Delta s_u / \Delta z}{\gamma_{\text{buoyant}}} \quad (1)$$

The value of γ_{buoyant} for the clay is $100 \text{ pcf} - 62.4 \text{ pcf} = 37.6 \text{ pcf}$. Thus, the value of s_u/p' is:

$$\frac{s_u}{p'} = \frac{8.6 \text{ psf per ft}}{37.6 \text{ pcf}} = 0.23 \quad (2)$$

which is a reasonable value for this normally consolidated clay.

These values provide a good basis for establishing undrained strength profiles in the clay. The undrained strength at the top of the clay is equal to 0.23 times the effective overburden pressure at the top of the clay, and the undrained strength increases with depth in the clay at a rate of 8.6 psf per foot.

In the IPET strength model, the undrained shear strength of the clay is equal to 0.23 times the effective overburden pressure. The clay strength thus varies with lateral position, being greatest beneath the levee crest where the effective overburden pressure is greatest, and varying with depth, increasing at a rate of 8.6 psf per foot at all locations. Figure 13 shows the calculated undrained shear strength variation in the interdistributary clay at the toe of the levee and beyond. Based on the available test data, the IPET

⁶ Mayne, P. W. (2003). "Class 'A' Footing Response Prediction from Seismic Cone Tests," Proceedings, Deformation Characteristics of Geomaterials, Vol. 1, Lyon, France.

strength model appears to be an adequate, albeit conservative, representation of the strength beneath the toe.

The IPET strength model does not consider details of the stress distribution beneath the levee, which would result in “load spread” effects. These effects would result in rotation of principal stresses beneath the levee, and in the added stress due to the levee load that would decrease with depth. Including these complex effects would complicate the model considerably. In our opinion, such refinement would make the model impractical, and is not justified. The model described in the previous paragraphs uses a simple stress distribution beneath the levee that satisfies vertical equilibrium, and it reflects the fact that the undrained strength is proportional to the effective consolidation pressure, certainly the most important aspect of the strength of the clay.

It is also important to note that the ground elevation of the toe of the levee is not constant; therefore it is not possible to use the same strength versus elevation relationship for the south breach and the north breach. The decrease in elevation of the toe from the south breach to the north breach is shown in the LIDAR survey of the area in the year 2000, which is plotted in Figure 14. The elevation of the protected side levee toe decreases about 4 ft from the south breach to the north breach.

The drained friction angle of the sand beneath the clay was estimated to be 30 degrees for the stability analysis. As noted previously, the sand layer is not involved in observed or computed failure mechanisms, and the value of ϕ' assigned to it, therefore, has no influence on computed factors of safety.

Original Design Strengths - East Bank

The design analyses in the Chalmette Area Plan General Design Memorandum (GDM)⁷ used undrained strengths for the levee fill, the marsh layers, and the clay, and a drained friction angle to characterize the strength of the sand layer beneath the clay, as does the IPET strength model described above. However, there are four marsh layers in the GDM interpretation compared to only two marsh layers for the IPET strength model. The design strengths are comparable to the IPET strengths discussed here and shown in Table 5 and Figure 15.

The values of strength for the levee fill, the marsh layers, and the clay layer that were used in the design analyses for the IHNC I-wall, Station 16+08.85 to Station 58+12.00, are shown in Table 5. This reach includes both breach areas on the east bank, which extends approximately from Stations 54+00 to 56+00 for the north breach and 22+00 to 31+00 for the south breach.

⁷ Design Memorandum No. 3, General Design, Lake Pontchartrain, LA, and Vicinity, Chalmette Area Plan, U.S. Army Engineer District, New Orleans, October 1966.

Table 5. Comparison of strengths of levee fill, marsh layers, and interdistributary clay used in design for Stations 16+08.85 to 58+12.00 with the IPET strengths.

Material	Strengths used for design	IPET strength model
Levee fill	$s_u = 500$ psf, $\phi = 0$	$s_u = 500$ psf, $\phi = 0$
Marsh 1a layer (uppermost marsh layer)	$s_u = 400$ psf, $\phi = 0$ beneath the levee and toe	$s_u = 650$ psf, $\phi = 0$ beneath levee $s_u = 550$ psf, $\phi = 0$ beneath toe
Marsh 1b layer (directly below uppermost marsh layer)	$s_u = 600$ psf, $\phi = 0$ beneath levee $s_u = 500$ psf, $\phi = 0$ beneath toe	
Marsh 2a layer (highly organic layer)	$s_u = 300$ psf, $\phi = 0$ beneath levee $s_u = 200$ psf, $\phi = 0$ beneath toe	$s_u = 300$ psf, $\phi = 0$ beneath levee $s_u = 200$ psf, $\phi = 0$ beneath toe
Marsh 2b layer (directly below marsh 2a layer)	$s_u = 500$ psf, $\phi = 0$ beneath levee $s_u = 300$ psf, $\phi = 0$ beneath toe	
Interdistributary Clay	12.3 psf/ft increase beneath levee (starting at 355 psf) 8 psf/ft increase beneath toe (starting at 300 psf)	$S_u/p' = 0.23$; 8.6 psf/ft increase both beneath levee and toe (starting value depends on depth of overburden)

A comparison between the GDM and IPET strength models is presented in Figures 16 and 17 for the GDM design cross section. Shown in Figure 16 is the shear strength profile under the crest of the levee (horizontal coordinate of 0 ft) used in the original design, and the shear strength profile calculated using the IPET model. The IPET strength model has higher shear strengths in the Marsh 1 layer, and the GDM strength model has higher strengths in the lower portion of the Marsh 2 layer. Both models show a linear increase in undrained shear strength in the interdistributary clay layer, with the rate of increase greater for the GDM model than the IPET model. The difference in the rate of increase can be partially attributed to the difference in unit weights used in each model. The GDM strength model assumes a unit weight of the clay of 102.4 pcf for the upper portion of the clay and 107 pcf for the lower portion of the clay. The IPET model uses a unit weight of 100 pcf for the clay. The higher unit weights used in the GDM strength model would produce a larger increase in undrained shear strength per foot than the IPET model for the same undrained strength ratio. In addition, based on the assumed unit weights and the rate of strength increase, the GDM model corresponds to a greater undrained strength ratio, from about 0.28 to 0.31.

The difference between the GDM and IPET strength model is more pronounced for undrained strengths below the toe of the levee. Shown in Figure 17 is the shear strength profile under the toe of the levee (horizontal coordinate of 60 ft) used in the original design, and the shear strength profile calculated using the IPET model. The

undrained shear strengths are comparable in the marsh layers, but there is about a 200 psf difference in undrained shear strength in the interdistibutary clay. The rate of increase for both models is essentially the same, but the IPET strength model produces a lower shear strength at the marsh/clay interface. As stated earlier, the IPET strength model appears to be conservative for undrained shear strengths beneath the toe when compared to available test data. This conservation was noted at a late stage in this investigation, when time was not available to change the interpretation.

It is interesting to note the similarity of the two strength models, particularly since the GDM strength model was developed about 40 years ago. Both models share the essential characteristics of using different strengths under the levee crest and toe, and a lateral variation of shear strengths between these points.

IHNC East Bank North and South Failures

Eighteen slope stability analyses (Cases 1 through 5, 5a, and 6 through 17 in Table 6) were performed for the cross section at Station 55+00 at the north breach. The cross section used for these analyses is shown in Figure 18. Also, 17 slope stability analyses (Cases 1 through 17 in Table 7) were performed for a cross section developed for Station 26+00 at the south breach. The cross section used for these analyses is shown in Figure 19.

In addition, four slope stability analyses (Cases 1 through 4 in Table 8) were performed using the cross section and strength profile shown in the GDM, and presented in this report as Figure 15.

Average values of moist unit weight were used in the analyses: $\gamma_{\text{sat}} = 109$ pcf for the levee fill, $\gamma_{\text{sat}} = 105$ pcf for the Marsh 1 layer, $\gamma_{\text{sat}} = 80$ pcf for the Marsh 2 layer, and $\gamma_{\text{sat}} = 100$ pcf for the interdistibutary clay beneath the marsh layers. These values are based on values measured in laboratory tests on undisturbed samples.

The critical slip surfaces found in the analyses did not extend down to the sand beneath the clay, and the sand strength and unit weight therefore did not influence the results of the analyses.

The analyses were performed for undrained conditions in the levee fill, the marsh layer, and the clay beneath the marsh layer. Based on available information, it appears that the values of permeability of all three of these materials were low enough so that dissipation of excess pore pressures during the rise of the water level in the canal would have been negligible, and would have had, at most, a minor influence on stability.

Analyses were performed for two conditions regarding contact between the I-wall and the adjacent soil on the canal side of the wall. These are indicated by “yes” or “no” in the column labeled “Crack” in Tables 6, 7 and 8.

- For the “no crack” analyses, it was assumed that the soil on the canal side of the wall was in intimate contact with the wall. Water pressures were applied to the surface of the levee fill, and to the I-wall where it projected above the crown of the levee, but were not applied to the face of the wall below the crown of the levee.

- For the “crack” analyses, it was assumed that the I-wall was separated from the levee fill on the canal side of the wall as the water level in the canal rose and caused the wall to deflect away from the canal. Full hydrostatic water pressures were applied to the I-wall, from the water level in the canal to the bottom of the wall.

For the north breach, stability analyses were performed for canal water elevations of 10.0, 10.5, 11.2, and 12.5 ft. Analyses were performed with water elevations of 10.0, 10.5, and 12.5 for the south breach. The elevation of the top of the wall is 12.5 ft for both the north and south cross sections.

The analyses described here were performed using the computer program UTEXAS4⁸. Critical circular slip surfaces were located for each case using the search routines available in UTEXAS4. The analyses were performed using Spencer’s method⁹, which satisfies all conditions of equilibrium. Methods that satisfy all conditions of equilibrium have been shown to result in values of factor of safety that are not influenced appreciably by the details of the assumptions they involve¹⁰.

⁸ Available from Shinoak Software, 3406 Shinoak Drive, Austin, TX 78731

⁹ Spencer, E. (1967) "A Method of Analysis of the Stability of Embankments Assuming Parallel Inter-Slice Forces," *Geotechnique*, Institution of Civil Engineers, Great Britain, Vol. 17, No. 1, March, pp. 11-26.

¹⁰ Duncan, J. M., and Wright, S. G. (2005), *Soil Strength and Slope Stability*, John Wiley and Sons, New York, 293 pp.

Table 6. Results of slope stability analyses for IHNC east bank, north breach. Note all analyses use Spencer's method and circular slip surfaces.

Case	Water Elev. Ft NAVD88	Strength Model	Crack (Yes or No)	Factor of Safety
1	10.0	IPET	Yes	1.04
2	10.5	IPET	Yes	1.03
3	10.5	IPET	No	1.22
4	11.2	IPET	Yes	1.00
5	12.5	IPET	Yes	0.96
5a	12.5	IPET	No	1.13
6	10.0	Marsh 1 + 25%	Yes	1.12
7	10.0	Marsh 1 - 25%	Yes	0.96
8	10.0	Marsh 2 + 25%	Yes	1.12
9	10.0	Marsh 2 - 25%	Yes	0.95
10	10.0	Interdistributary + 25%	Yes	1.12
11	10.0	Interdistributary - 25%	Yes	0.94
12	12.5	Marsh 1 + 25%	Yes	1.04
13	12.5	Marsh 1 - 25%	Yes	0.88
14	12.5	Marsh 2 + 25%	Yes	1.05
15	12.5	Marsh 2 - 25%	Yes	0.88
16	12.5	Interdistributary + 25%	Yes	1.03
17	12.5	Interdistributary - 25%	Yes	0.88

Table 7. Results of slope stability analyses for IHNC east bank, south breach. Note all analyses use Spencer's method and circular slip surfaces.

Case	Water Elev. Ft NAVD88	Strength Model	Crack (Yes or No)	Factor of Safety
1	10.0	IPET	Yes	1.20
2	10.5	IPET	Yes	1.18
3	10.5	IPET	No	1.34
4	12.5	IPET	Yes	1.10
5	12.5	IPET	No	1.25
6	10.5	Marsh 1 + 25%	Yes	1.29
7	10.5	Marsh 1 - 25%	Yes	1.07
8	10.5	Marsh 2 + 25%	Yes	1.27
9	10.5	Marsh 2 - 25%	Yes	1.09
10	10.5	Interdistributary + 25%	Yes	1.27
11	10.5	Interdistributary - 25%	Yes	1.07
12	12.5	Marsh 1 + 25%	Yes	1.21
13	12.5	Marsh 1 - 25%	Yes	1.00
14	12.5	Marsh 2 + 25%	Yes	1.18
15	12.5	Marsh 2 - 25%	Yes	1.02
16	12.5	Interdistributary + 25%	Yes	1.18
17	12.5	Interdistributary - 25%	Yes	1.01

Formation of a crack on the canal side of the wall, allowing hydrostatic water pressure acting through the full depth of the crack, causes a very significant reduction in the value of the calculated factor of safety. Evidence that a crack did form behind the wall near the breaches can be seen in Figures 6 and 7.

For the north breach (Station 55+00), with the canal water level at elevation 12.5 ft (top of the wall), the calculated factor of safety for the cracked condition is 0.96, as compared to 1.13 for the uncracked condition (Cases 5 and 5a). A canal water elevation of 11.2 ft produces a factor of safety of unity for the cracked condition (Case 4). Figures 20 through 25 show the critical circles from UTEXAS4 analyses for the north breach for Cases 1 through 5 and Case 5a.

For the south breach (Station 26+00), the factor of safety was greater than unity for all canal water elevations analyzed using the IPET strength model. For the most extreme case of the canal water level at elevation 12.5 ft (top of the wall), the calculated factor of safety for the cracked condition is 1.10. The critical circles for the stability analyses performed on the south breach for Cases 1 through 5 are shown in Figures 26 through 30.

Analysis of GDM Cross section

An analysis of the design cross section was performed using the GDM strength model discussed earlier. This analysis allows a comparison of the Method of Planes, used in the original design, with Spencer's method using circular failure surfaces.

In the original design, a canal water level of 10.5 ft NAVD88 (13.0 ft NGVD29) was used as the design water level load condition. The Method of Planes resulted in a minimum factor of safety of 1.25 for a horizontal failure plane located in the Marsh 2 layer. Using Spencer's method with the GDM strength model, a factor of safety of 1.45 was calculated for the same canal water level. Thus, the Method of Planes is conservative by about 14% in this case.

Three other variations of the design cross section were analyzed. Introducing a crack behind the wall for the design water level decreases the factor of safety to 1.19. For a canal water elevation at the top of the wall (12.5 ft NAVD88), the factor of safety is 1.35 for the uncracked condition and 1.05 for the cracked condition. The results of all analyses performed on the GDM cross section are presented in Table 8. Figures 31 through 34 show the critical circles for the UTEXAS4 analysis.

Probabilities of Failure

Probabilities of failure have been estimated using an approximate technique based on the Taylor Series method. The coefficient of variation of the average clay strength and the average marsh layer strength were estimated to be 25%. The data available is sparse, and the scatter in measured values is influenced significantly by sample quality, as well as variations in properties from one location to another and systematic variations with depth over burden. The estimated values of COV = 25% is, thus, largely based on judgment. Even so, it is useful to examine what probabilities of failure would be associated with this level of uncertainty concerning shear strengths.

The Taylor Series numerical method¹¹, was used to estimate the standard deviation of the factor of safety (σ_F) and the coefficient of variation of the factor of safety (COV_F), using these formulas:

$$\sigma_F = \sqrt{\left(\frac{\Delta F_{\text{clay strength}}}{2}\right)^2 + \left(\frac{\Delta F_{\text{marsh strength}}}{2}\right)^2} \quad (3)$$

$$COV_F = \frac{\sigma_F}{F_{MLV}} \quad (4)$$

where $\Delta F_{\text{clay strength}}$ = difference between the values of the factor of safety calculated with the clay strength increased by one standard deviation and decreased by one standard deviation from its most likely value. $\Delta F_{\text{marsh strength}}$ is determined in the same way. F_{MLV} is the “most likely value” of factor of safety, computed using the IPET shear strengths.

Values of F_{MLV} and COV_F have been calculated for Station 55+00 and for Station 26+00. The results are listed in Table 9, together with the corresponding values of probability of instability based on an assumed lognormal distribution of factor of safety.

For Station 55+00, the calculated probabilities of instability are 42% for a water level of 10.0 ft, and 64% for the water level at the top of wall (12.5 ft, NAVD 88). For Station 26+00, the calculated probabilities of instability are 15% for the design water level of 10.5 ft, and 27% for a water level of 12.5 ft (top of wall). These values are reasonable, considering that evidence suggest that the north breach occurred before the wall overtopped and the south breach more likely failed due to overtopping.

Table 8. Results of slope stability analyses for IHNC East Bank, using GDM No. 3, Plate 38. Note all analyses use Spencer’s method with critical circles.

Case	Water Elev. Ft. NAVD88	Strength Model	Crack (Yes or No)	Factor of Safety
1	10.5**	GDM	No	1.45
2	10.5**	GDM	Yes	1.19
3	12.5 – Top of Wall	GDM	No	1.35
4	12.5 – Top of Wall	GDM	Yes	1.05

Note: Design WL is 2.0 ft below top of wall

¹¹Wolff, T. F. (1994). "Evaluating the reliability of existing levees." Report, Research Project: Reliability of Existing Levees, prepared for the U.S. Army Engineer Waterways Experiment Station, Geotechnical Laboratory, Vicksburg, MS.

Table 9. Calculated probabilities of instability for IHNC east bank

Area	Water level (ft) NAVD88	F _{MLV}	COV _F	Probability of instability
North Breach	10.0	1.04	14%	42%
North Breach	12.5	0.96	15%	64%
South Breach	10.5	1.18	15%	15%
South Breach	12.5	1.10	14%	27%

F_{MLV} = most likely value of factor of safety

COV_F = coefficient of variation of factor of safety

West Bank North and South Breaches

Observations

Two breaches occurred on the west bank of the IHNC, as shown in Figure 1. Both breaches occurred north of the railroad gate on France Road and just east of the France Road crossing.

The northern breach, between Stations 195+00 and 196+40¹², occurred after the I-wall at that location was overtopped, and soil supporting the wall was removed by erosion. The water elevation of the top of the wall was 12.5 ft, 1.7 ft lower than the peak elevation reached in the IHNC. A cross section through the levee and the I-wall is shown in Figure 35.

The southern breach, between stations 0+80 and 2+80¹³, occurred when the levee at that location was overtopped and eroded. There was no I-wall in this levee reach. The elevation of the top of the levee was 12.5 ft. A cross section through the levee is shown in Figure 36.

The levees at both locations were founded on about 8 ft to 10 ft of fill. The fill at the north breach was clay. At the south breach the fill consisted partly of silty sand and partly of clay, as shown in Figure 36. At both locations the fill was underlain by a layer of marsh material, about 11 to 12 ft thick, and a layer of normally-consolidated intertributary clay 30 to 35 ft thick.

The shear strengths used in the stability analyses of the breached sections are summarized in Table 10. These values are based on data from the GDMs and from post-Katrina investigations.

¹² Design Memorandum No. 2 – General, Supplement No. 8, Lake Pontchartrain, LA and Vicinity, Lake Pontchartrain Barrier Plan, Inner Harbor Navigation Canal Remaining Levees, Office of the District Engineer, New Orleans District, Corps of Engineers, February, 1968.

¹³ Modification of Protected Alignment and Pertinent Design Information, IHNC Remaining Levees, West Levee Vicinity, France Road and Florida Avenue Containerization Complex, Office of the District Engineer, New Orleans District, Corps of Engineers, October, 1971. Note: A different stationing origin was used for the two sections in the GDMs. The location of the south section would correspond to Stations 208+00 to 210+00 in the stationing system used for the north section.

Results of Stability Analyses – West Bank – North Breach

Stability analyses of the north breach section were performed using UTEXAS4⁸ for canal water elevations of 12.0 ft (the design water elevation) and 12.5 ft (the top of the wall). Analyses were performed for the cracked condition and the no-crack condition. For the cracked condition, the water-filled gap extended to the bottom of the sheetpile, elevation -12.5 ft. The factors of safety calculated in these analyses are listed in Table 11. It can be noted that the factors of safety for the cracked and the un-cracked conditions are the same. This occurs because, even with the crack, the critical slip circle passes beneath the tip of the sheet pile. If the slip circle is forced to intersect the gap at the bottom of the sheetpile, the calculated factor of safety increases.

These analyses show that the wall would have a considerable margin of safety against instability, even with the water at the top of the wall and a crack at the back of the wall. It thus seems highly likely that wall would have remained stable if none of the supporting soil had been removed by overtopping erosion.

Results of Stability Analyses – West Bank – South Breach

Stability analyses of the south breach section were performed using UTEXAS4⁸ for a canal water elevation of 12.5 ft (the top of the levee). The factor of safety for this condition was found to be 2.08. The concept of a gap does not apply to this section since there is no sheet pile wall on or in the embankment. The high factor of safety indicates that the breach was the result of erosion of the levee.

Summary

Four breaches occurred on the IHNC, two on the east bank, and two on the west bank. Three of the breaches involved failures of floodwalls on levees, and one involved failure of a levee without a floodwall.

The peak storm surge elevation in the IHNC was 14.2 ft at 9:00 AM on August 29, about 1.7 ft above the tops of the floodwalls and levees. Water flowing over the walls when they were overtopped eroded trenches on the protected side of the walls as it cascaded onto the levee fill, and soil that was providing support for the walls was removed by this erosion, making the walls less stable.

It is clear that one of the east side breaches occurred before the wall was overtopped, because eyewitness reports indicate that the water level in the 9th Ward near Florida Avenue was rising when the water level in the IHNC was still below the top of the floodwall. Stability analyses indicate that foundation failure would occur before overtopping at the north breach on the east side of the IHNC. This breach location is thus the likely source of the early flooding in the 9th Ward. Stability analyses indicate that the other three breach locations would not have failed before they were overtopped.

The failure that resulted in the north breach on the east side of the IHNC resulted from two differences between the stability analyses that were used as the basis for design and those described in this report: (1) the ground surface beyond the toe of the levee at the north breach location was lower than the landside ground surface in the design cross

section, and (2) the design analyses did not consider the possibility of a crack forming behind the wall, allowing water to run into the gap and increase the load on the wall.

Table 10. Shear strength parameters used in stability analyses of north and south breach locations on the IHNC west bank.

Unit	Unit Weight (pcf)	Shear Strength
Levee Fill	109	$\phi = 0$ $s_u = 500$ psf
Fill (Clay)	105	$\phi = 0$ $s_u = 500$ psf
Fill (Sand)*	120	$\phi' = 30^\circ$ $c' = 0$
Marsh	80	Toe: $\phi = 0$ $s_u = 200$ psf Crest: $\phi = 0$ $s_u = 300$ psf
Interdistributary Clay	100	Calculated using $s_u/p' = 0.27$

*Only present under south breach

Table 11. Results of Slope Stability Analyses of the IHNC West Bank North Breach.

Case	Water Elev. Ft NAVD88	Strength Model	Crack (Yes or No)	Factor of Safety
1	12.0	IPET	Yes	1.75
2	12.0	IPET	No	1.75
3	12.5	IPET	Yes	1.73
4	12.5	IPET	No	1.73

Note – analyses performed using Spencer’s Method with circular slip surfaces.

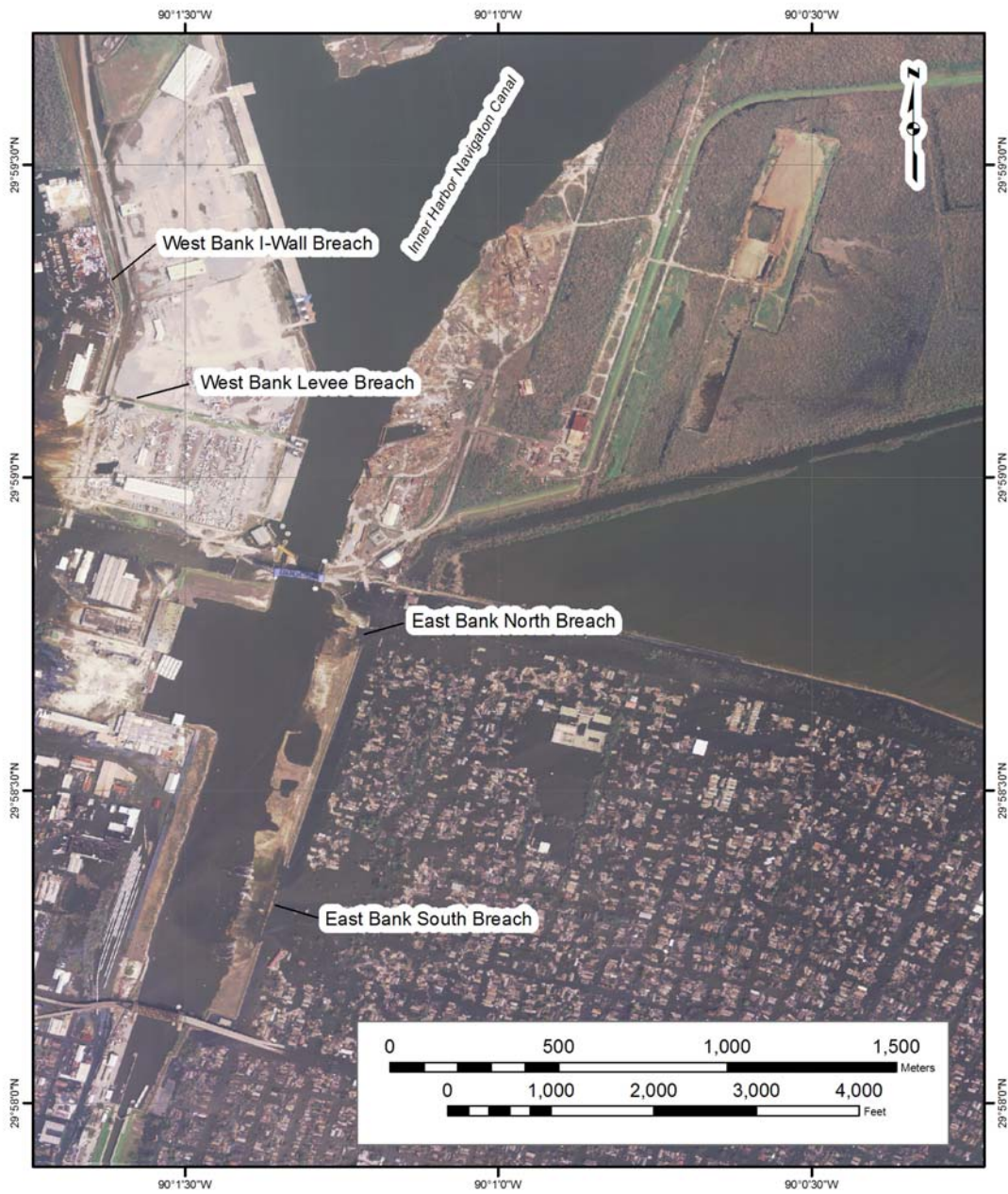


Figure 1. Four Breach Locations on the Inner Harbor Navigation Canal.

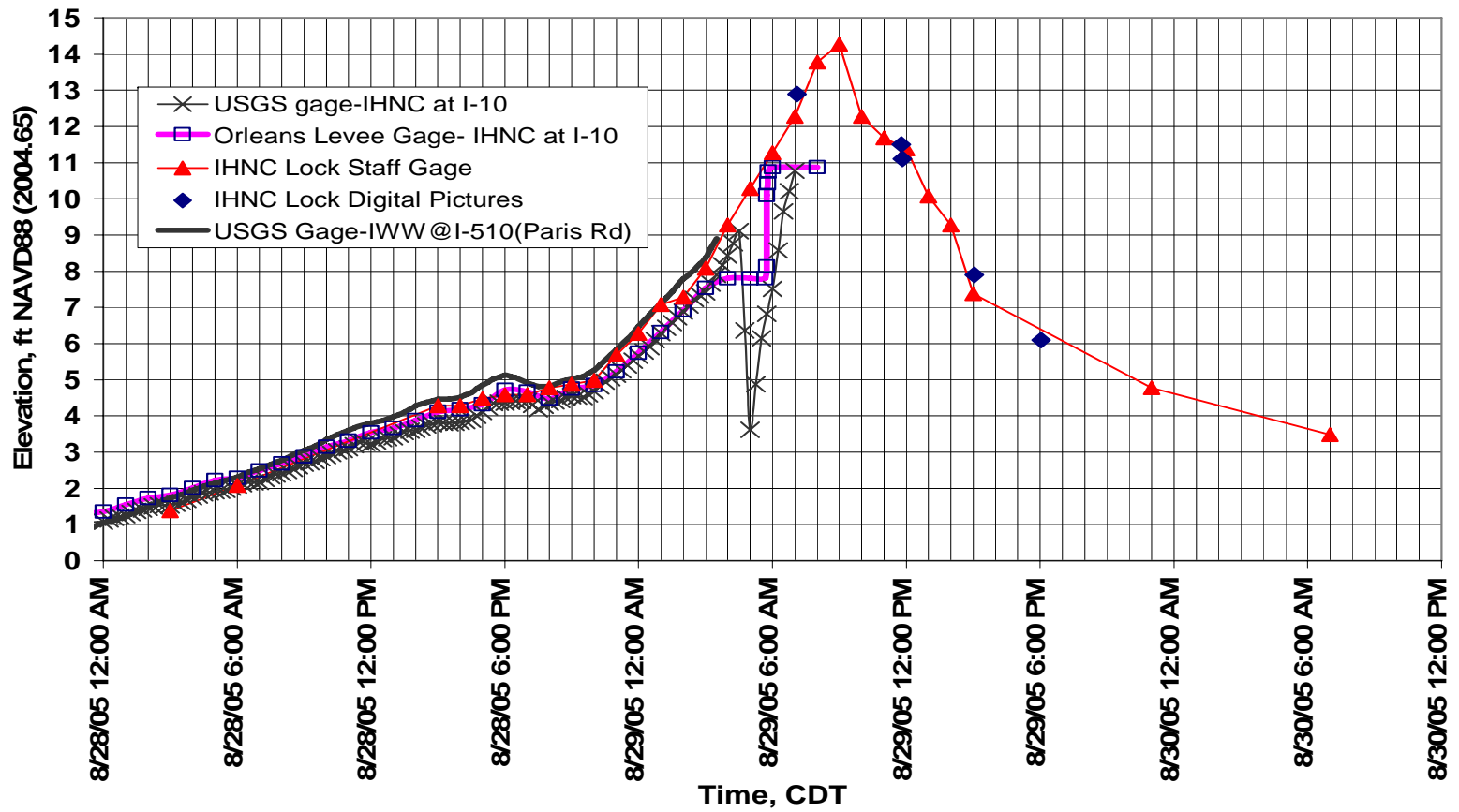


Figure 2. Katrina Hydrograph for the Inner Harbor Navigation Canal.

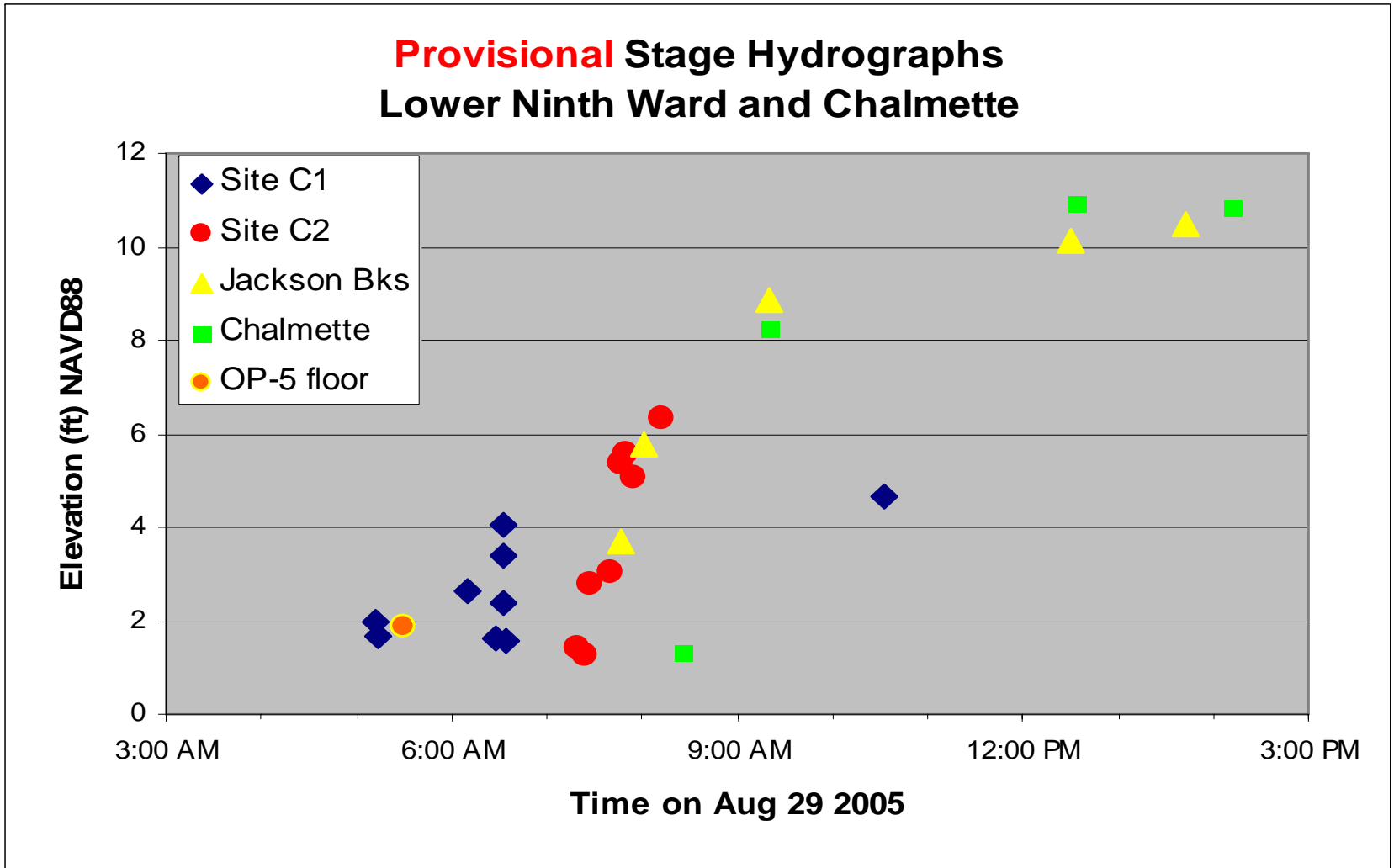


Figure 3. Hydrograph for the 9th Ward Inundation.



Figure 4. Scour and erosion on the protected side of the IHNC adjacent to the 9th Ward in the vicinity of the south breach.



Figure 5. Scour and erosion leading to the failure of the I-wall on the IHNC adjacent the south breach (9th Ward).



Figure 6. IHNC East Bank – South Breach – Wall movement.



Figure 7. IHNC East Bank – North Breach – Wall movement (View looking south)

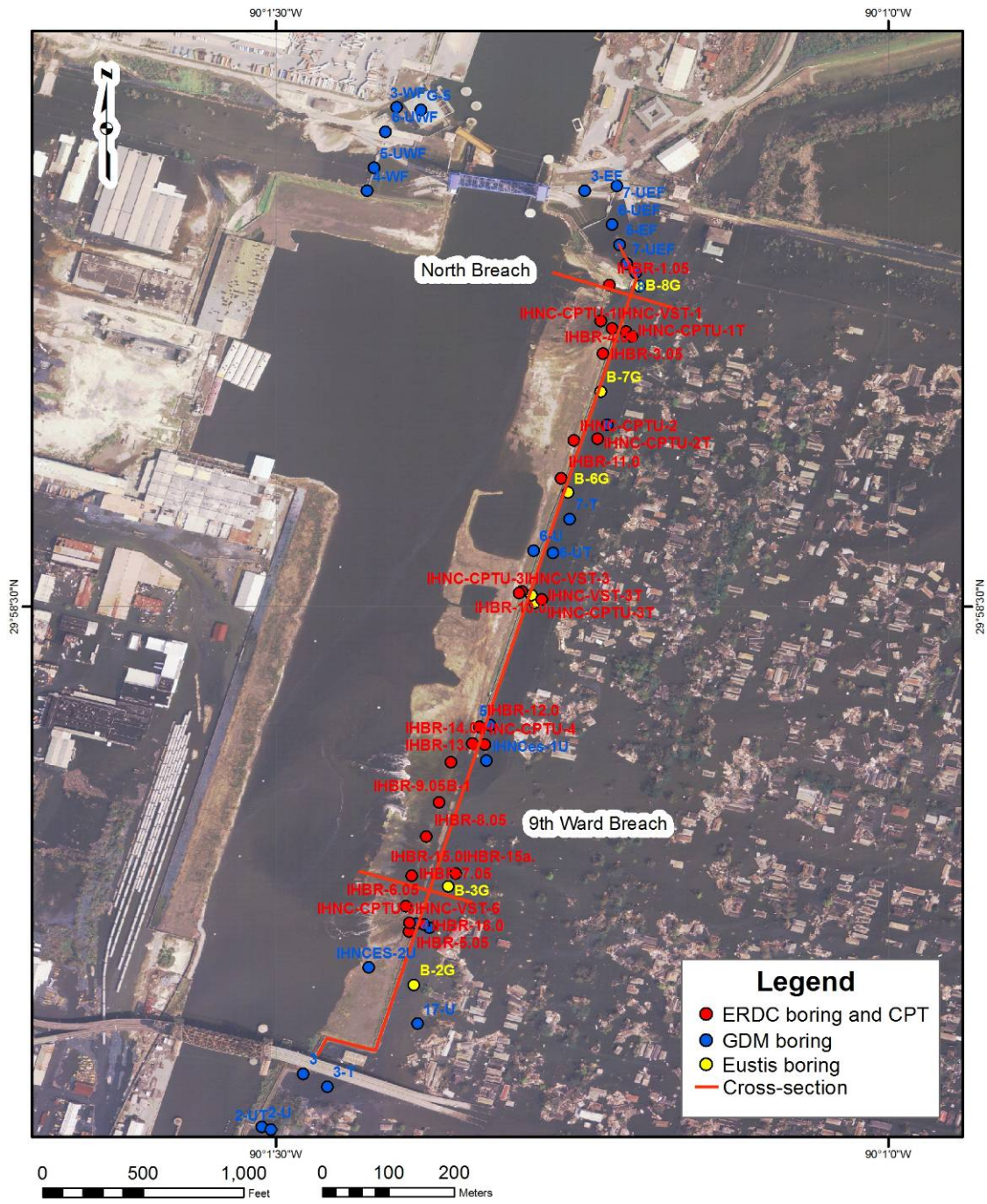
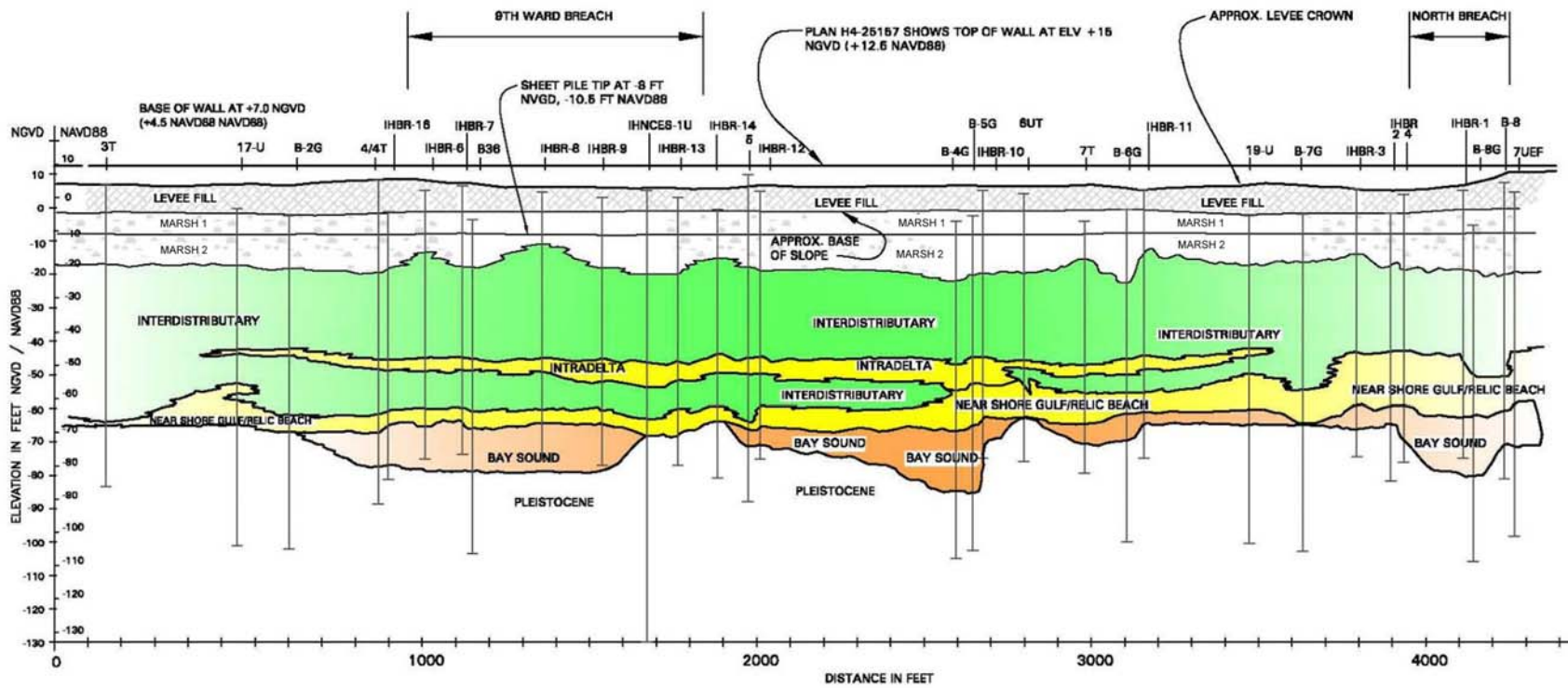


Figure 8. IHNC – East Bank (Between Florida Ave. and North Claiborne Ave.), Boring and CPTU Location Map.



IHNC EAST
CL PROFILE
 VIEW LOOKING WEST
 5-10-2008

Figure 9. IHNC East bank, centerline geologic section showing south (9th ward) and north breaches.

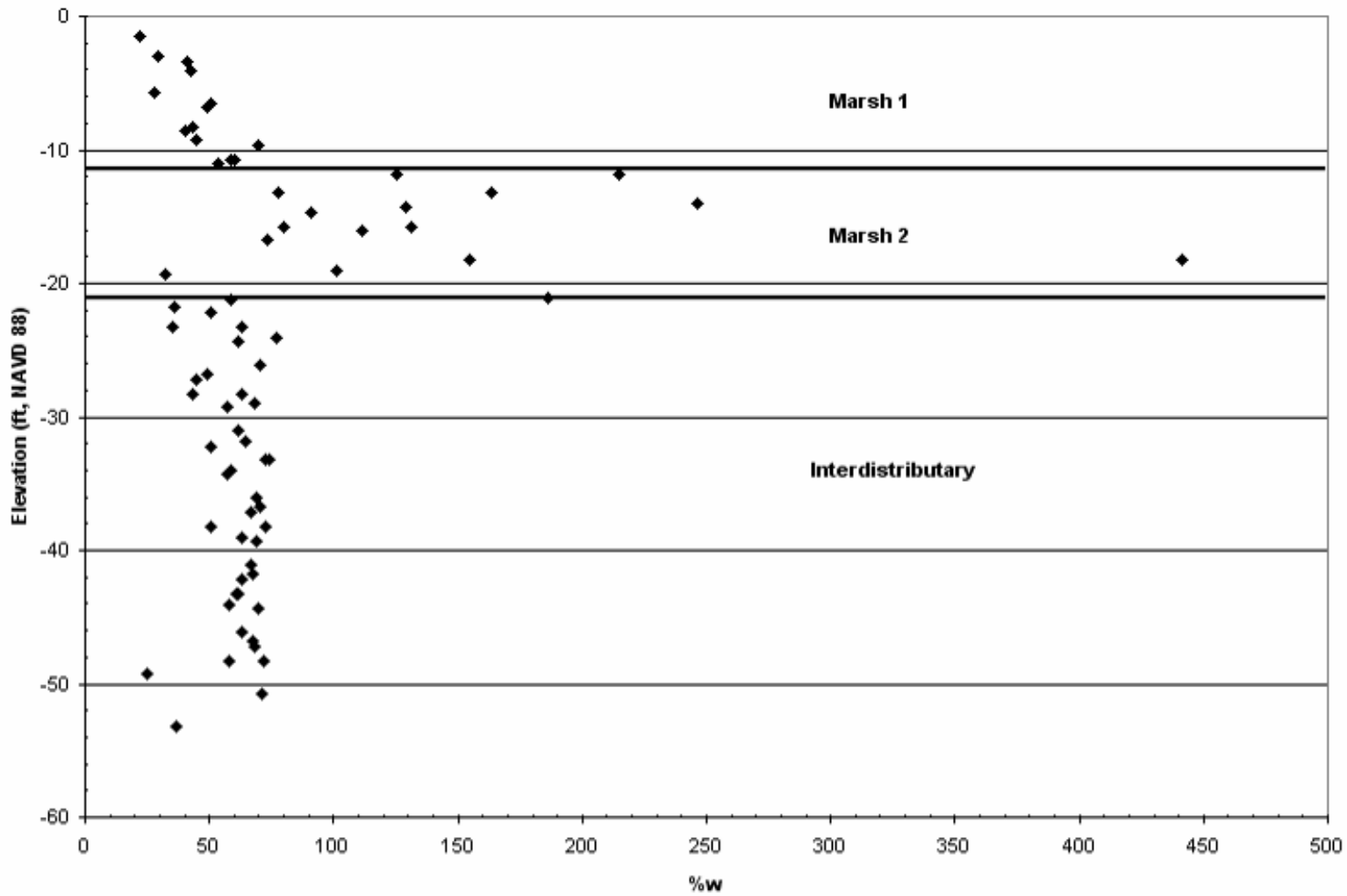


Figure 10. IHNC – East Bank (Between Florida Ave. and North Claiborne Ave.), % w versus Elevation (ft, NAVD 88), from toe borings

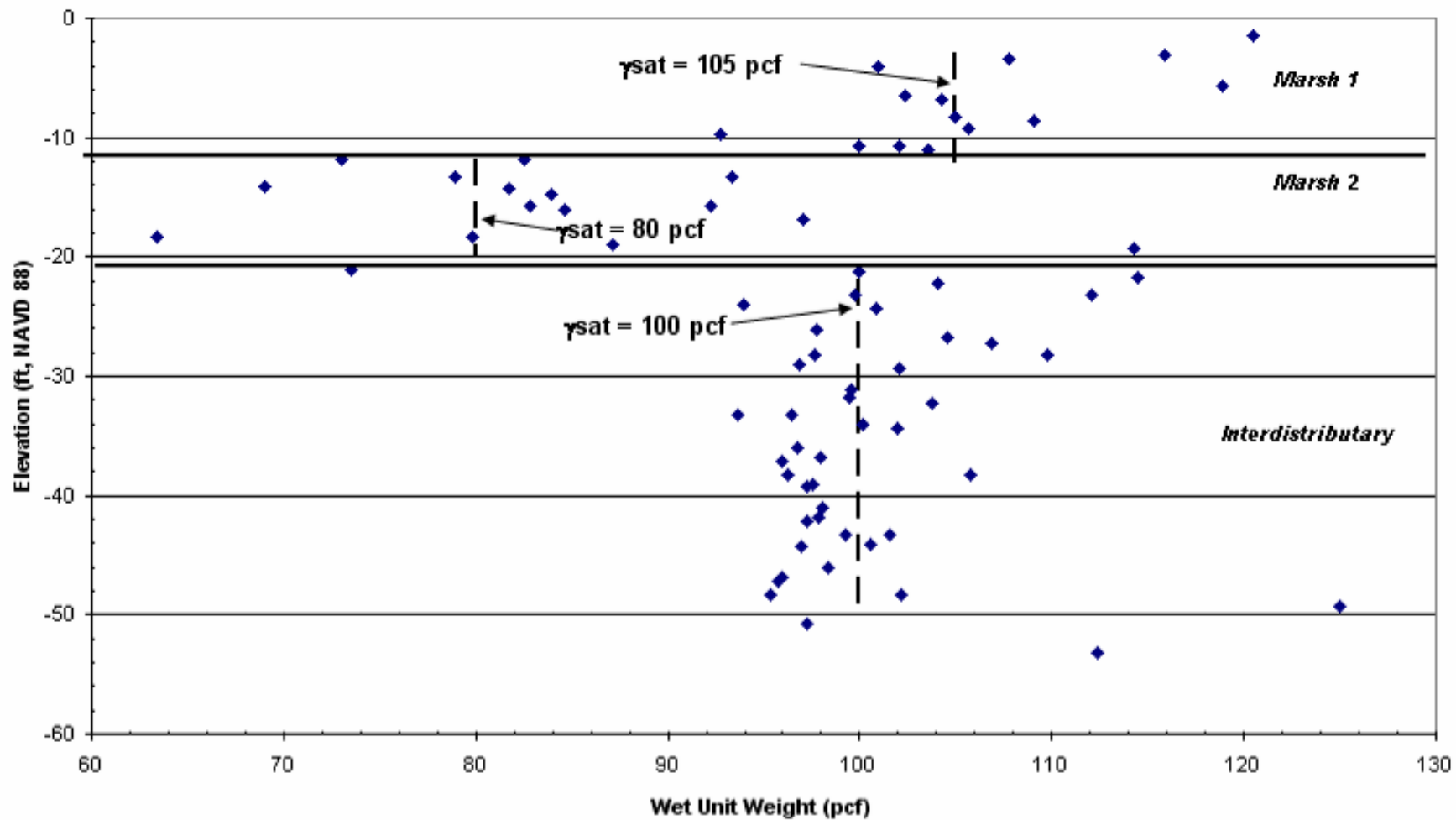


Figure 11. IHNC – East Bank (Between Florida Ave. and North Claiborne Ave.), Wet Unit Weight versus Elevation (ft, NAVD 88) from Post-Katrina borings

Shear Strength under Centerline

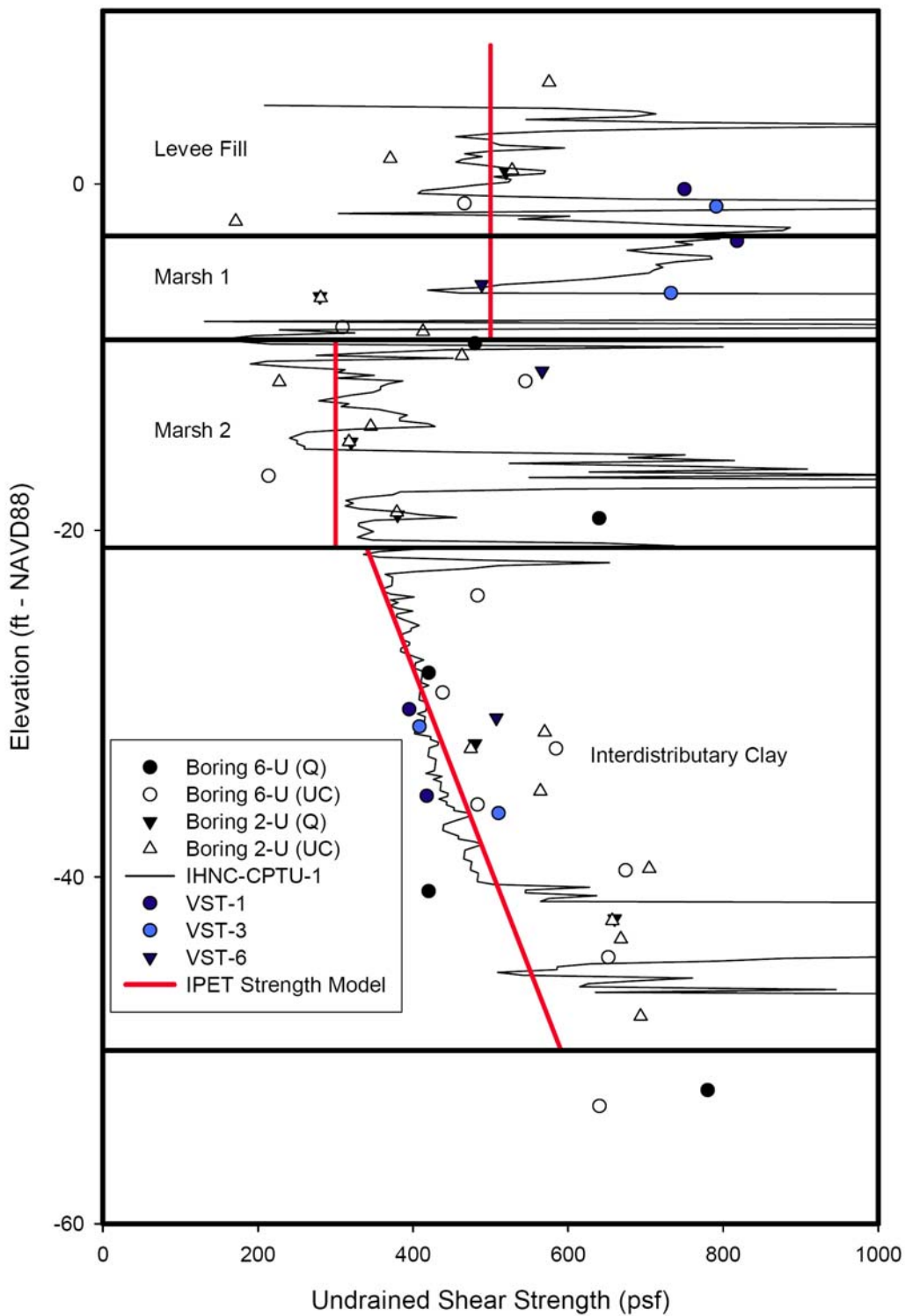


Figure 12. IHNC – East Bank laboratory and field shear strength results for the centerline of the levee.

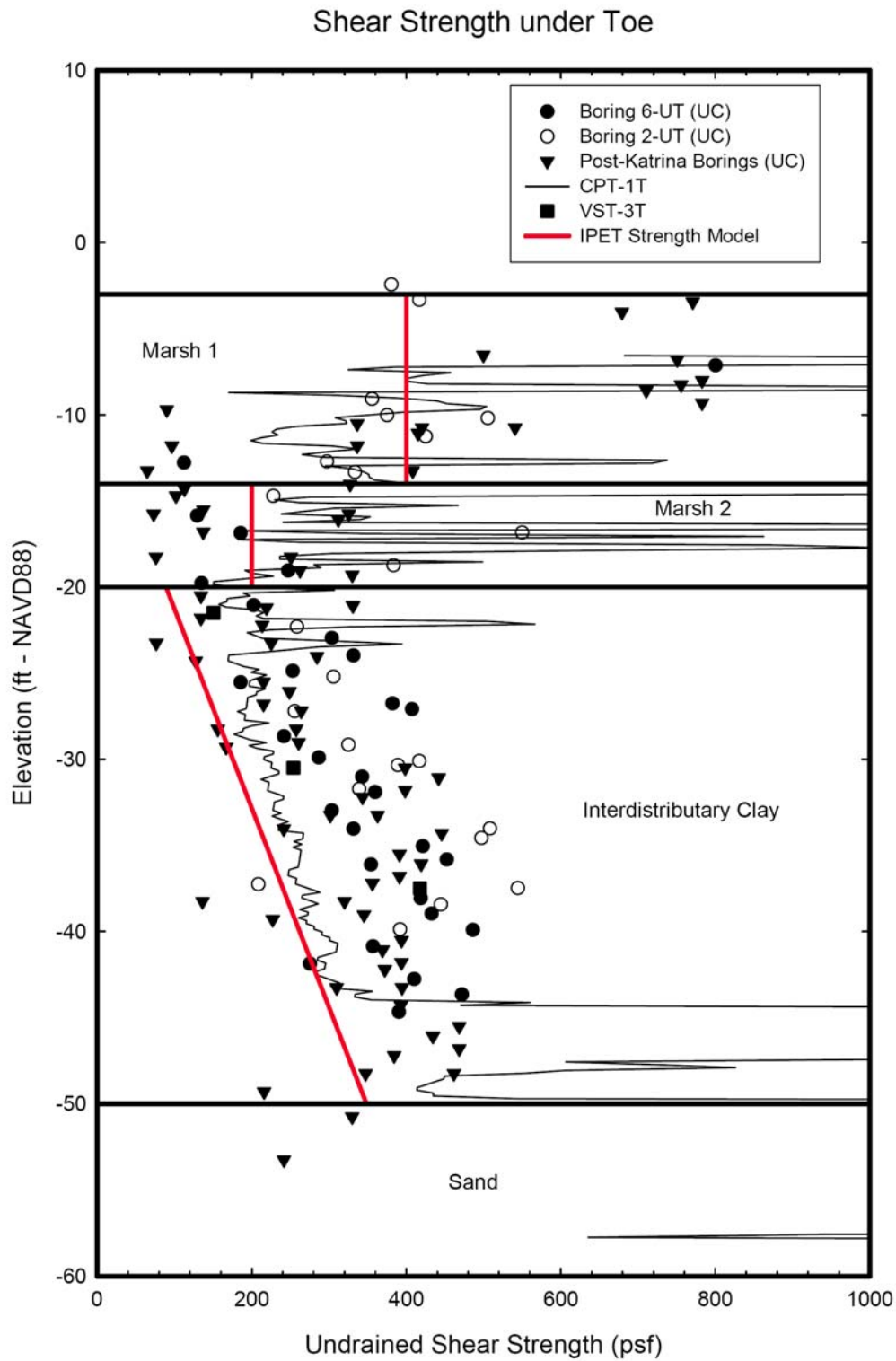


Figure 13. IHNC – East Bank laboratory and field shear strength results for toe of levee and beyond.

IHNC East Toe Profile

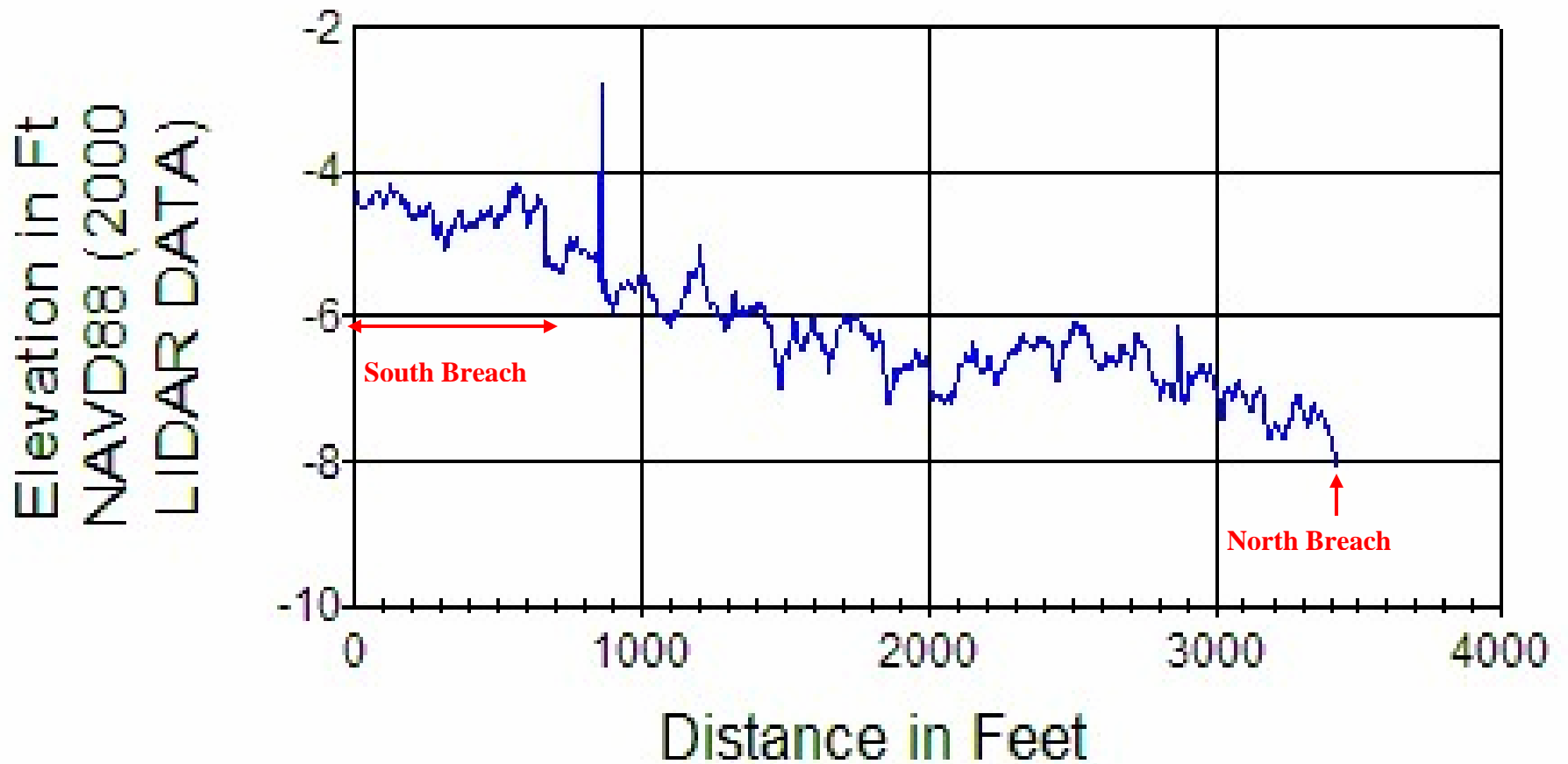


Figure 14. LIDAR data at toe of levee.

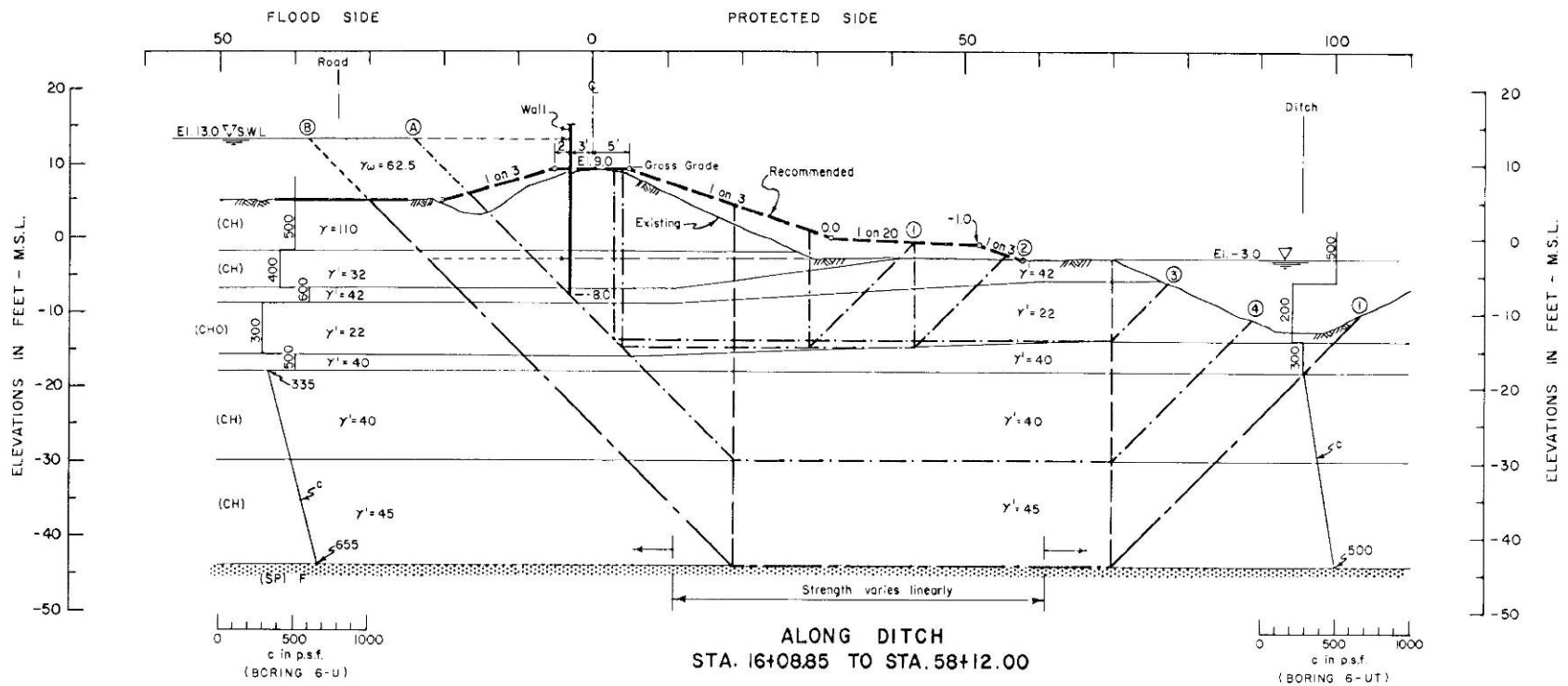


Figure 15. Cross section used for design for stations 16+09 to 58+12. Both east bank breaches occurred between these two stations.

Strength Distribution under Centerline (GDM cross section)

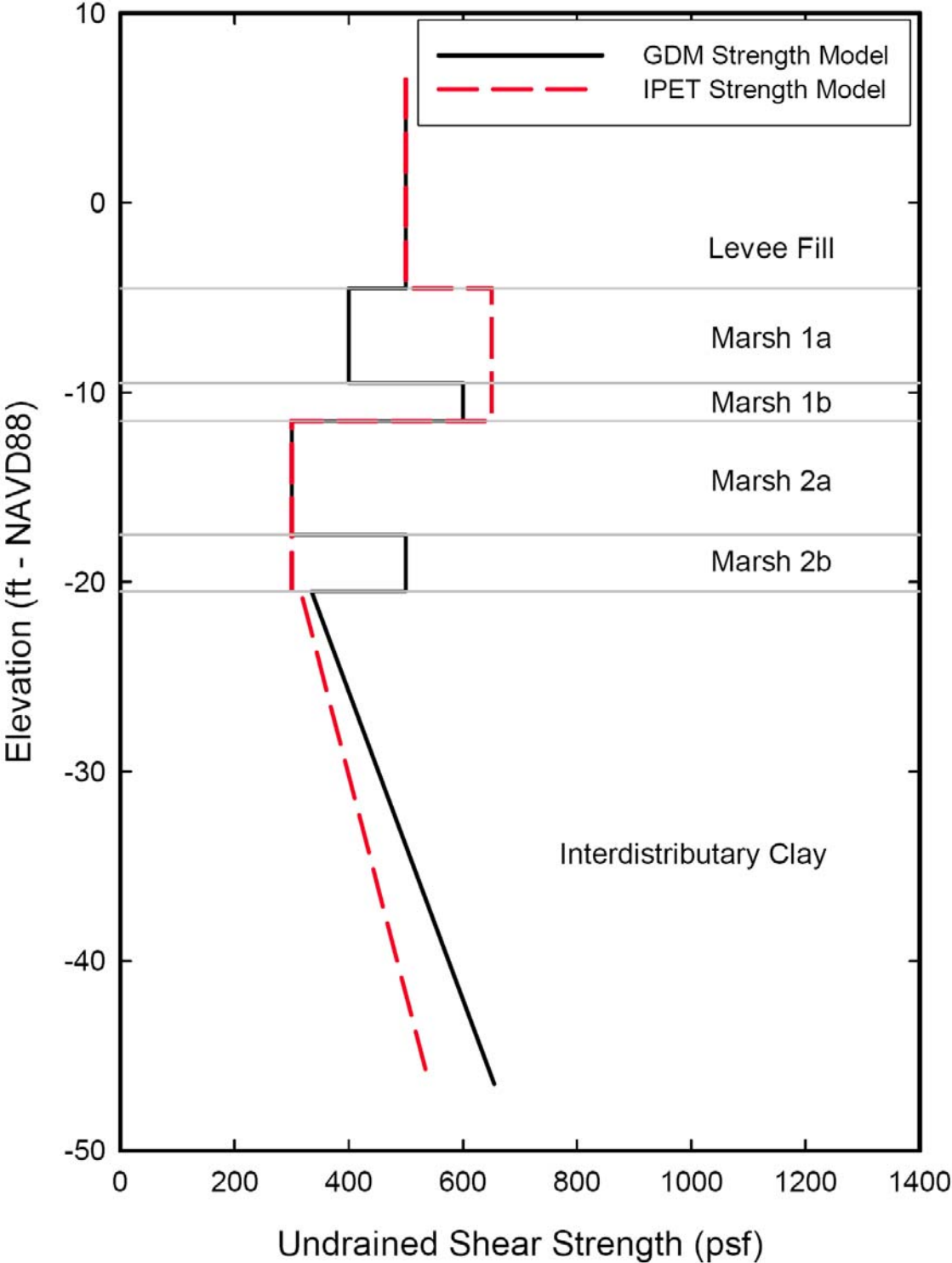


Figure 16 Comparison of GDM and IPET shear strength models for GDM design cross section at the centerline (horizontal coordinate of 0 ft in Figure 15).

Strength Distribution under Toe (GDM cross section)

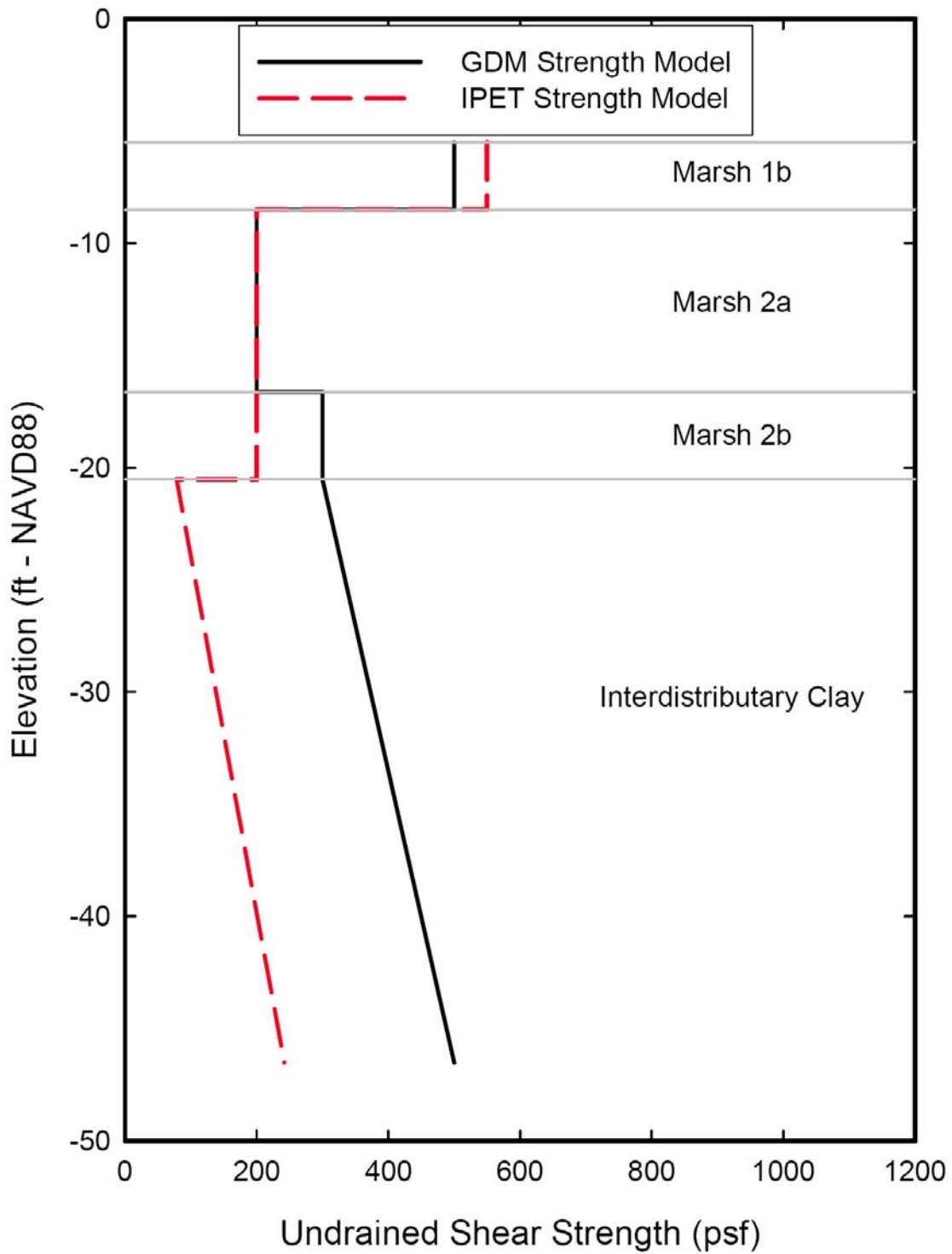


Figure 17 Comparison of GDM and IPET shear strength models for GDM design cross section at the toe (horizontal coordinate of 60 ft in Figure 15).

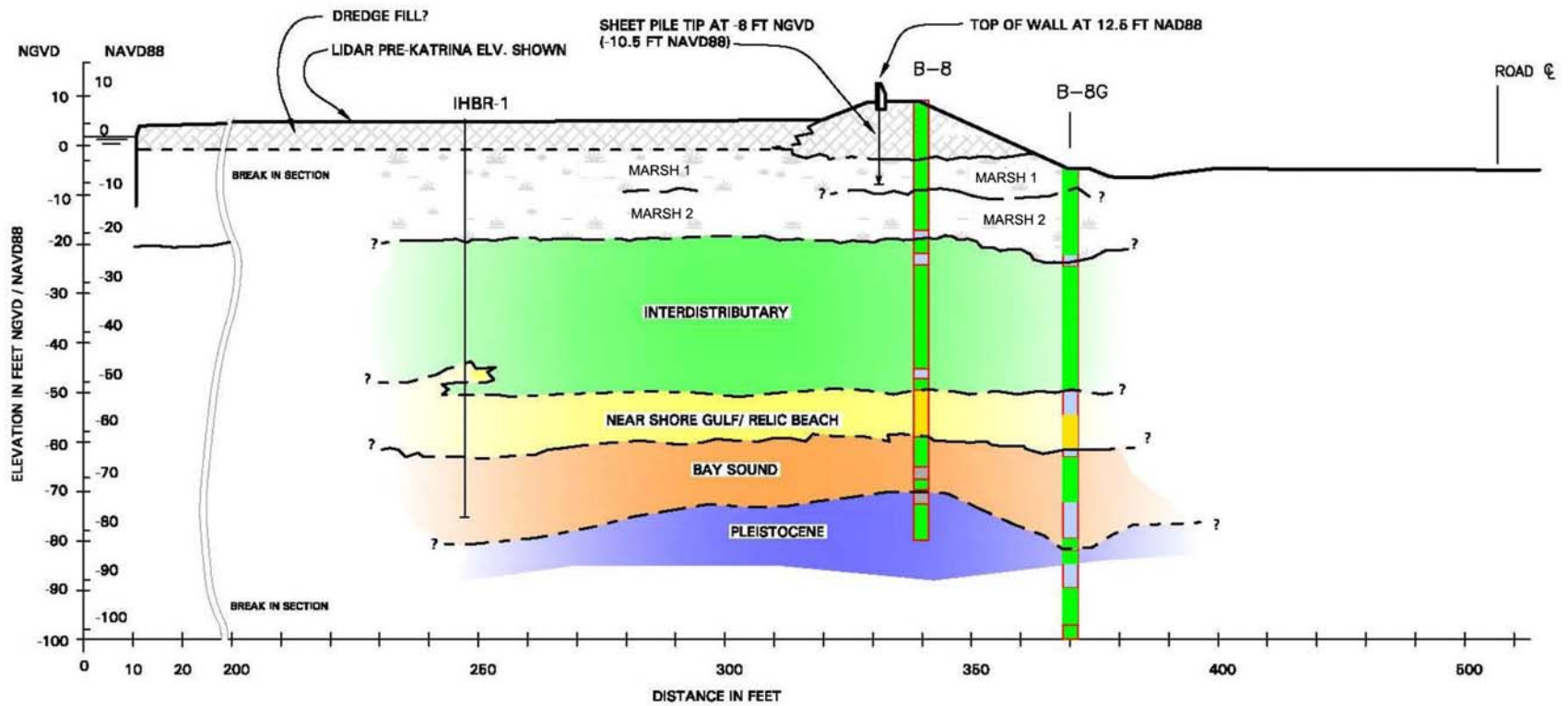


Figure 18. Profile of the north breach at IHNC East bank, view looking North

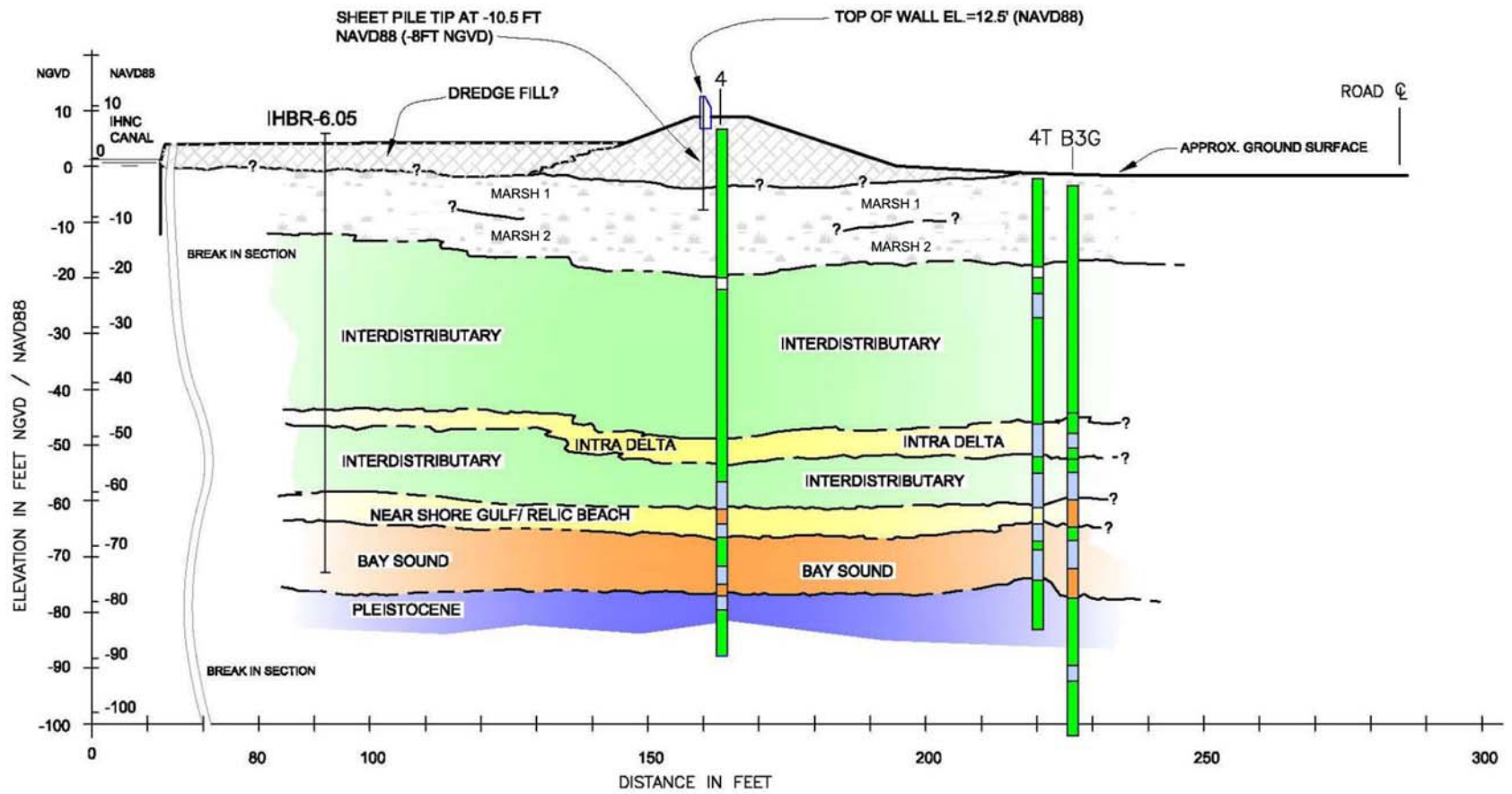


Figure 19. Profile of the south (9th Ward) breach at IHNC East bank, view looking North.

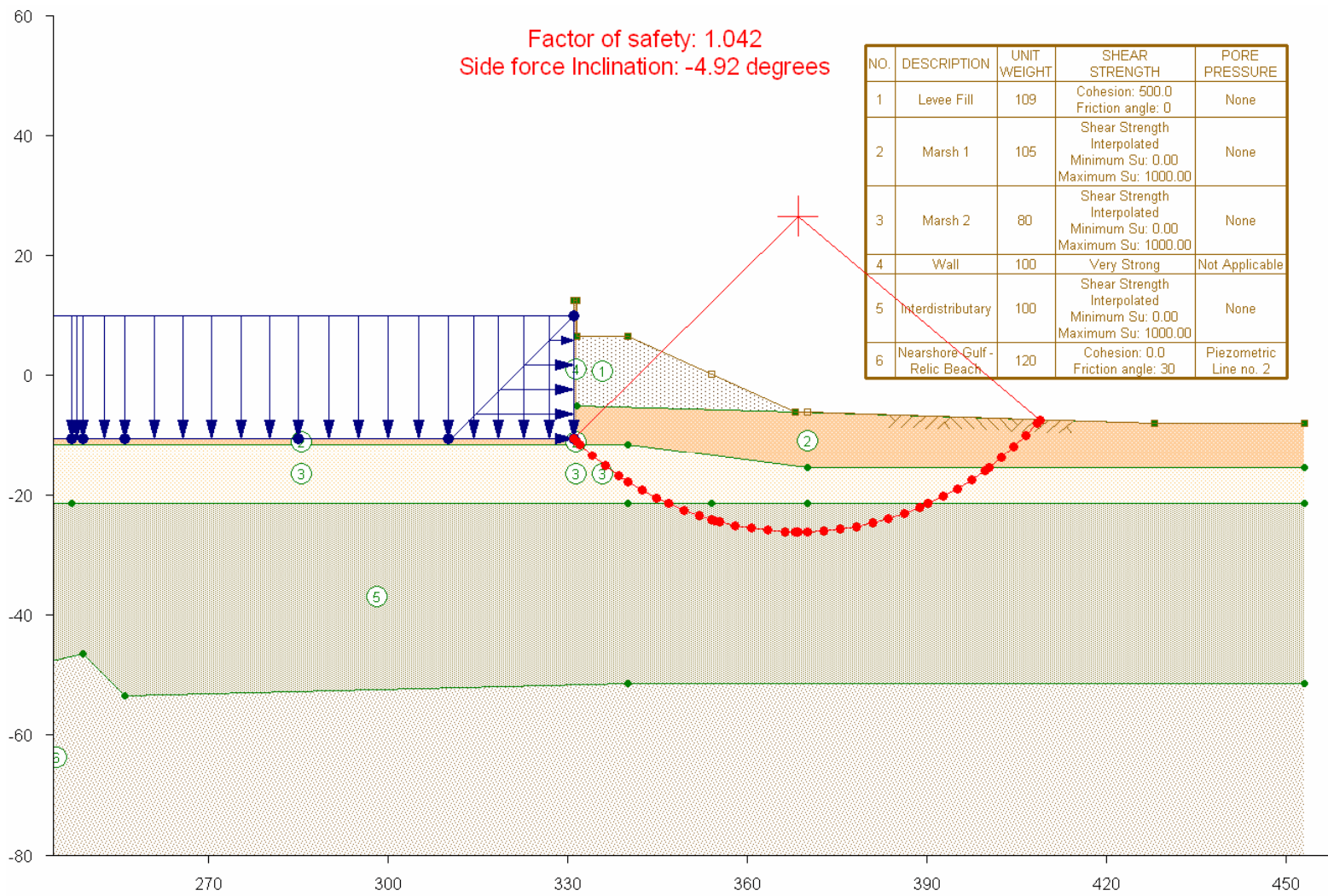


Figure 20. IHNC – East Bank (North Breach), Case 1, Canal Water Level = 10.0 ft (NAVD 88), with Crack

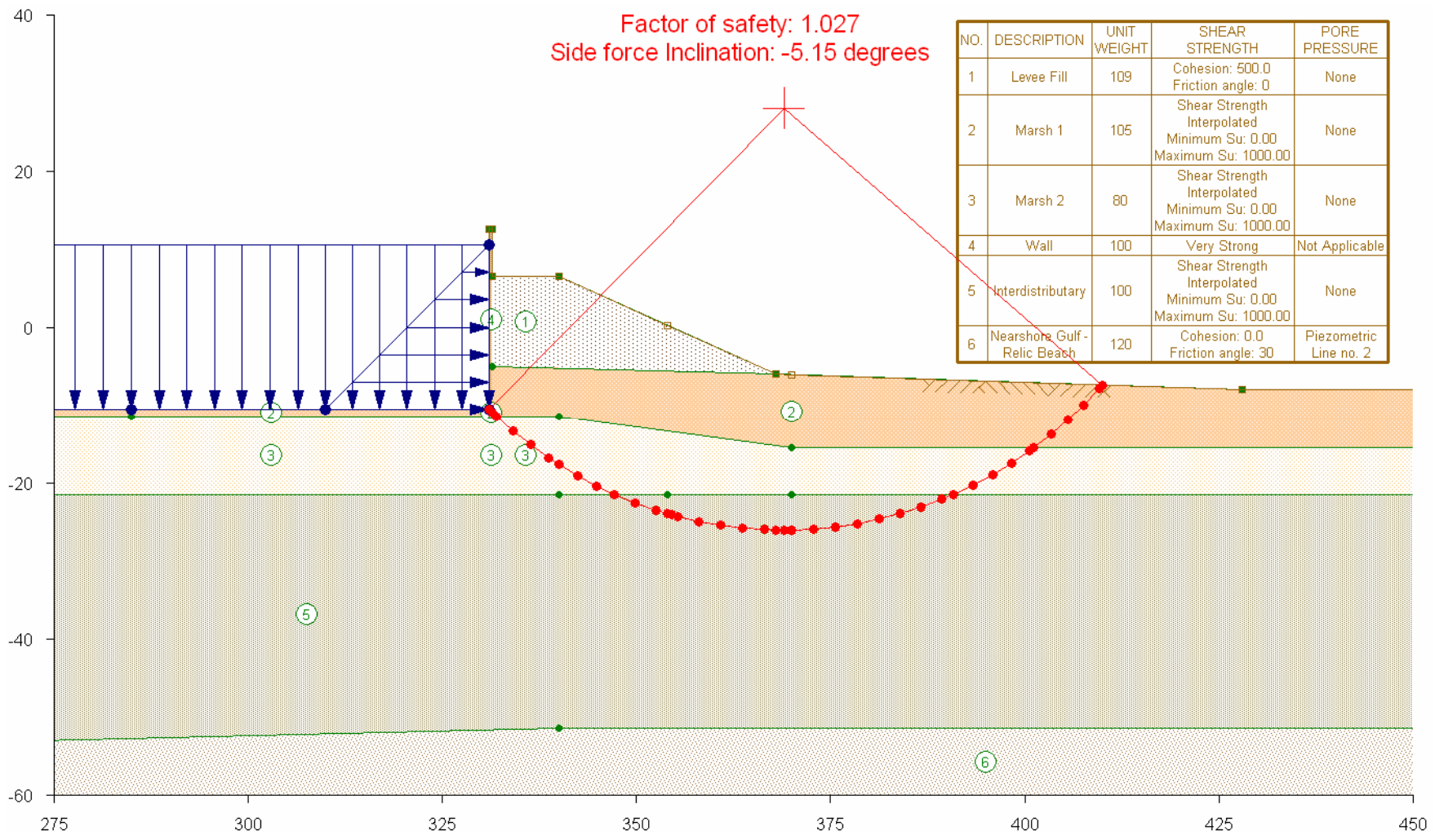


Figure 21. IHNC – East Bank (North Breach), Case 2, Design Canal Water Level = 10.5 ft (NAVD 88), with Crack

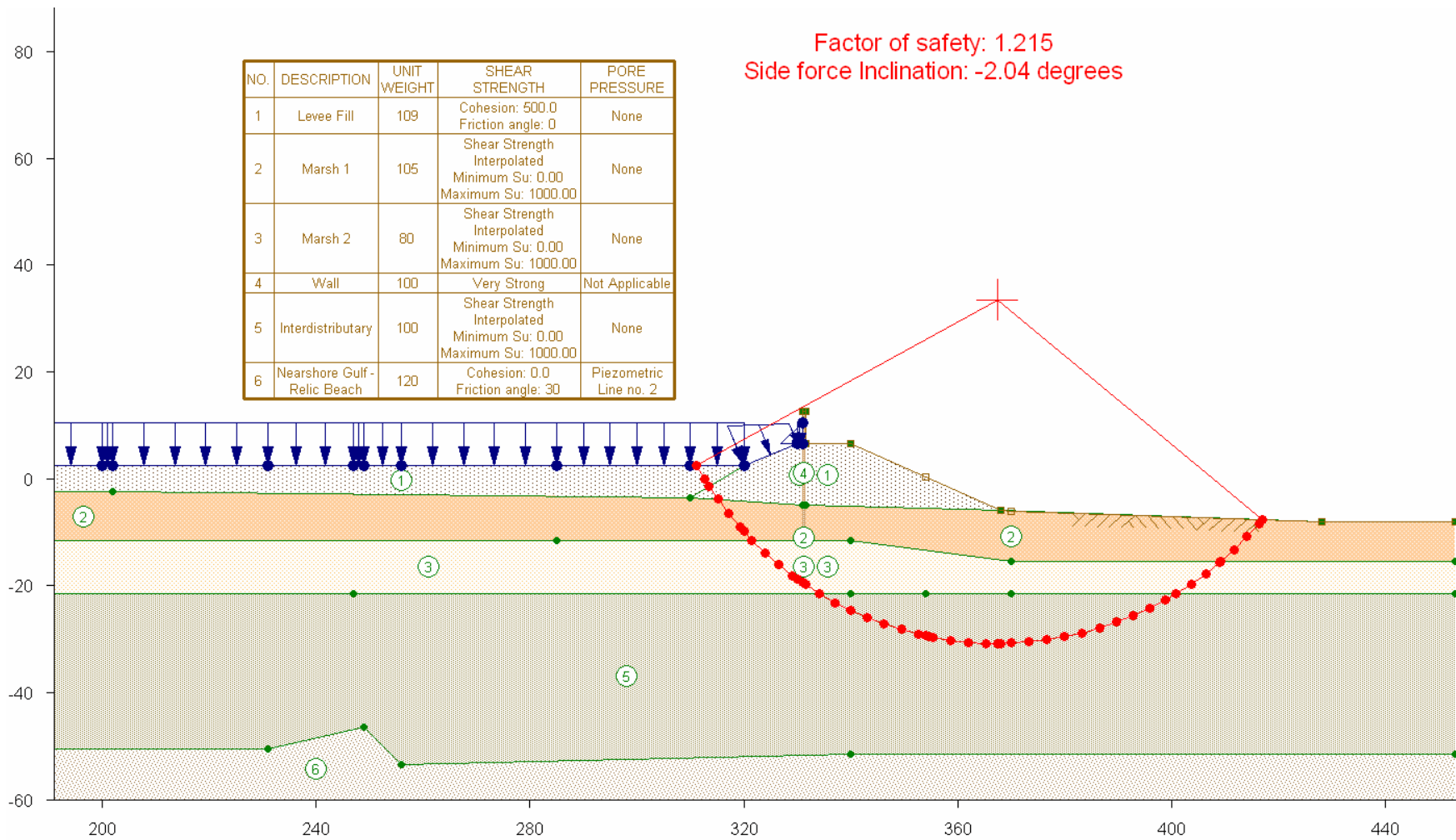


Figure 22. IHNC – East Bank (North Breach), Case 3, Design Canal Water Level = 10.5 ft (NAVD 88), without Crack

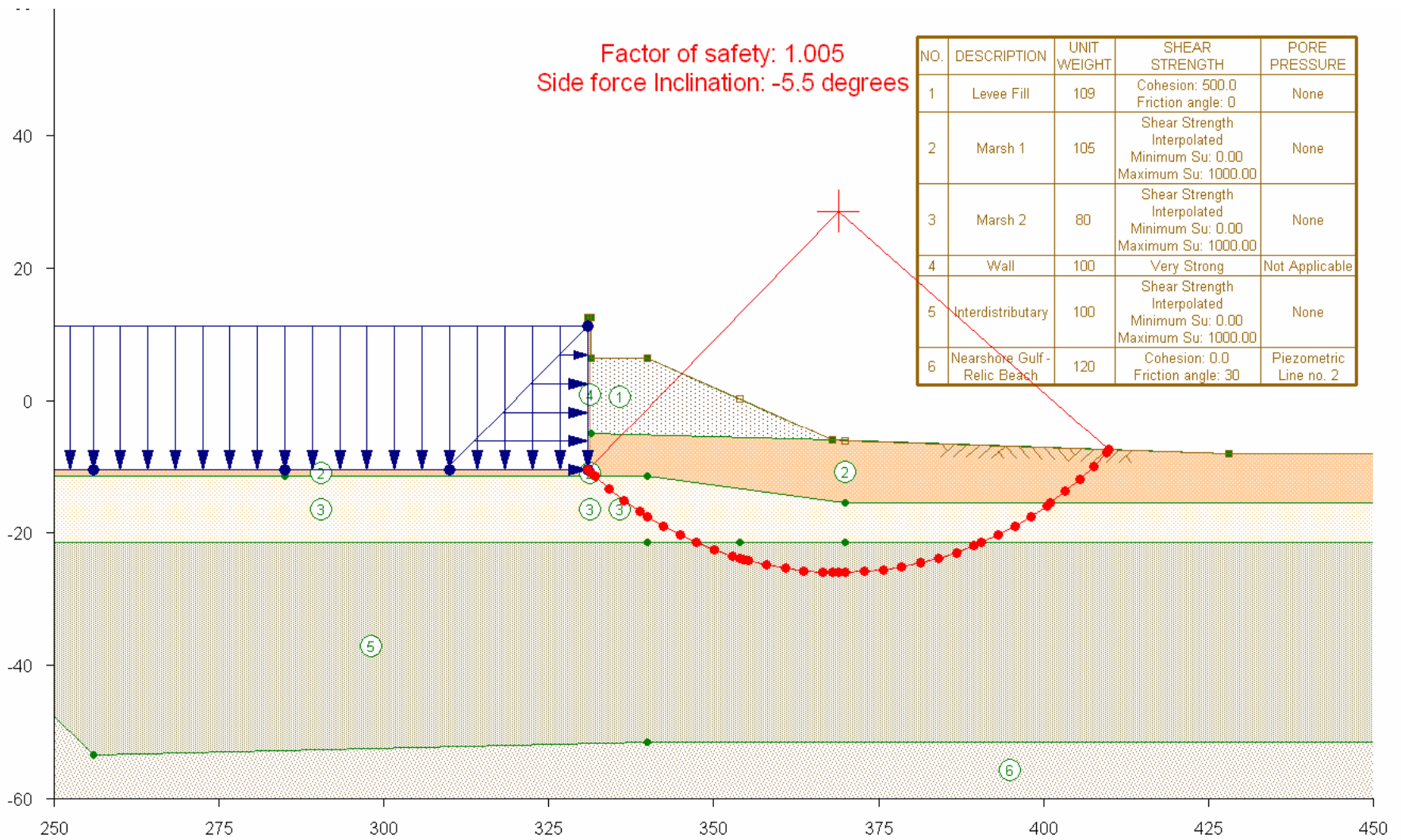


Figure 23. IHNC – East Bank (North Breach), Case 4, Canal Water Level = 11.2 ft (NAVD 88), with Crack

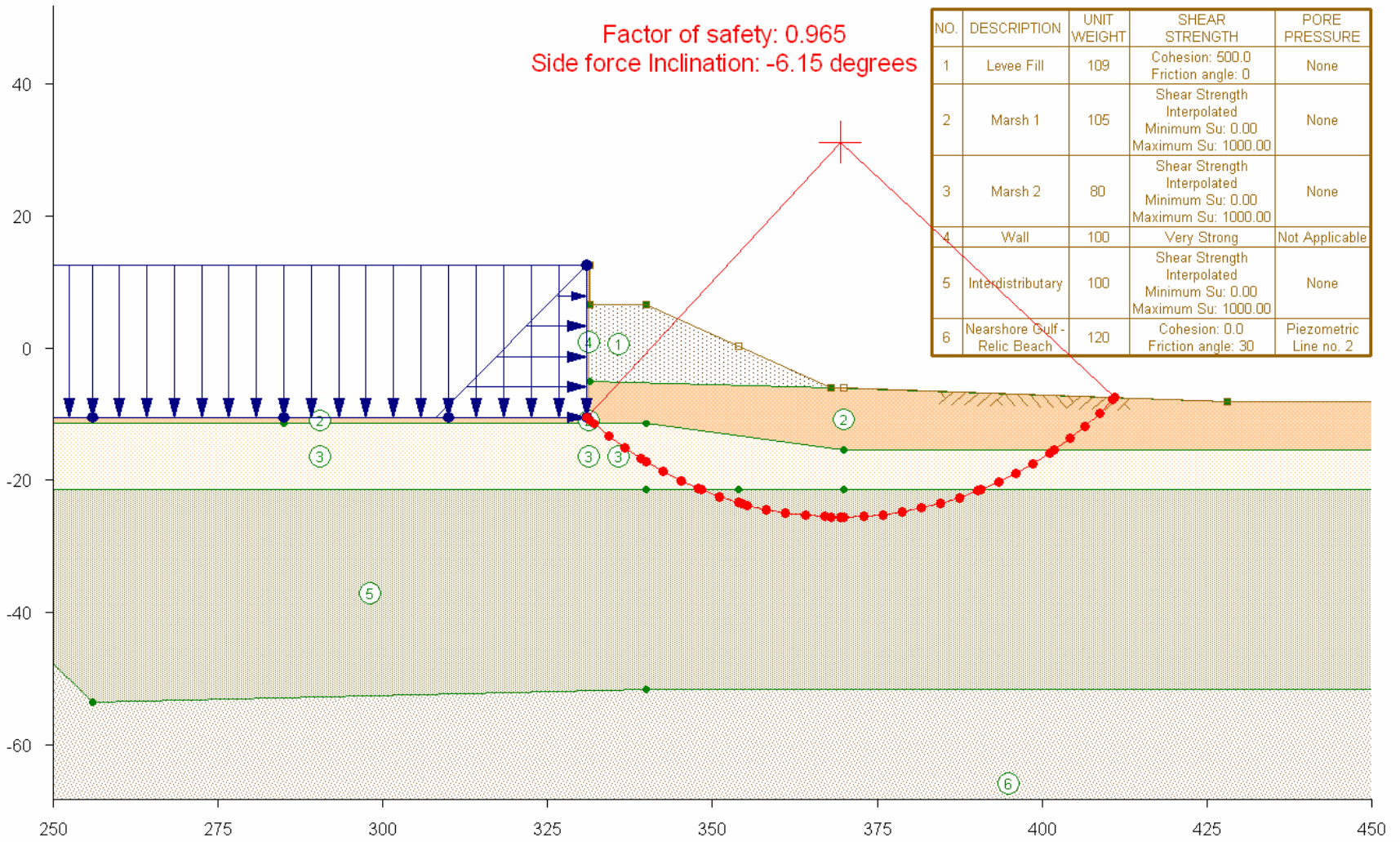


Figure 24. IHNC – East Bank (North Breach), Case 5, Canal Water Level = Top of Wall = 12.5 ft (NAVD 88), with Crack

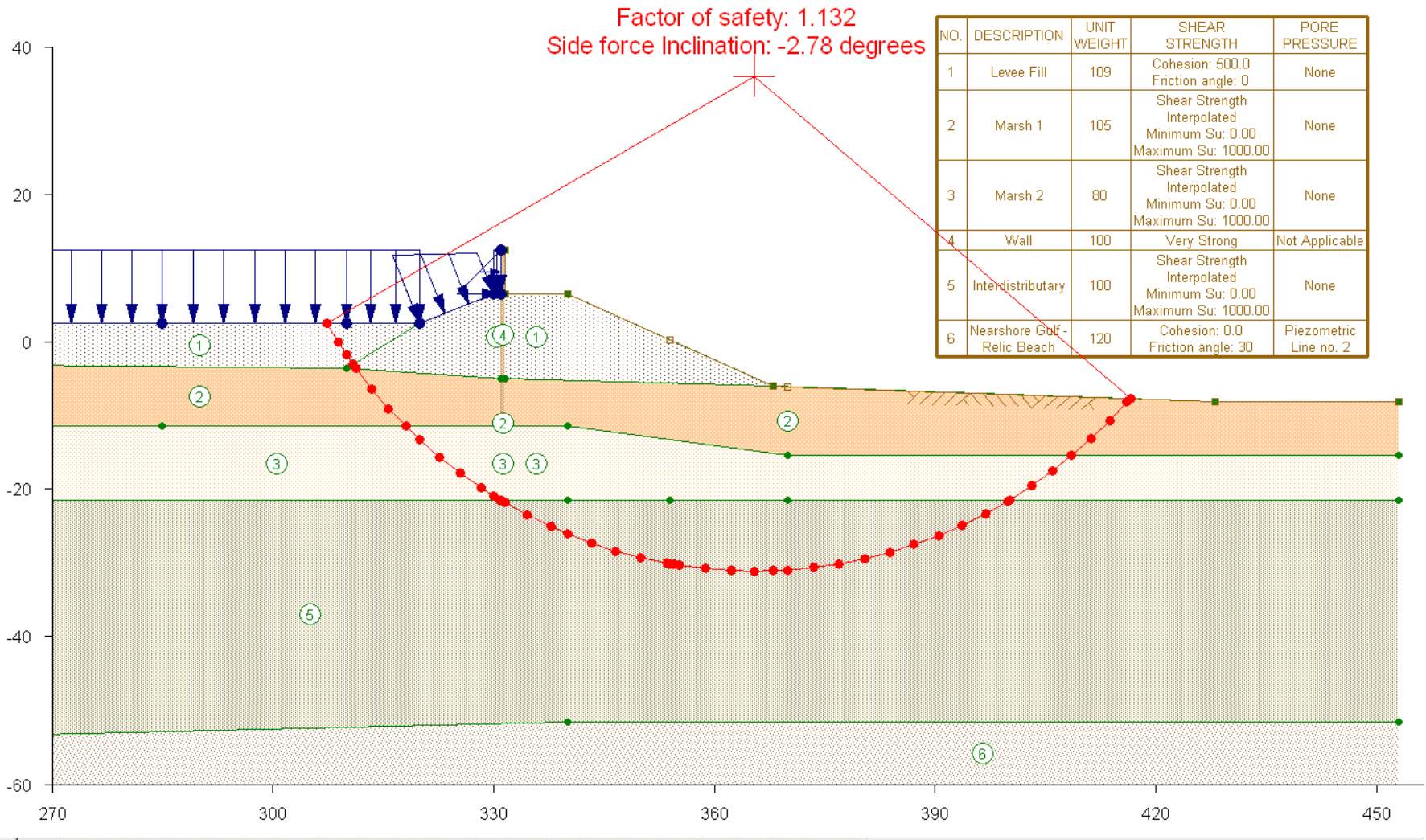


Figure 25. IHNC – East Bank (North Breach), Case 5a, Canal Water Level = Top of Wall = 12.5 ft (NAVD 88), without Crack

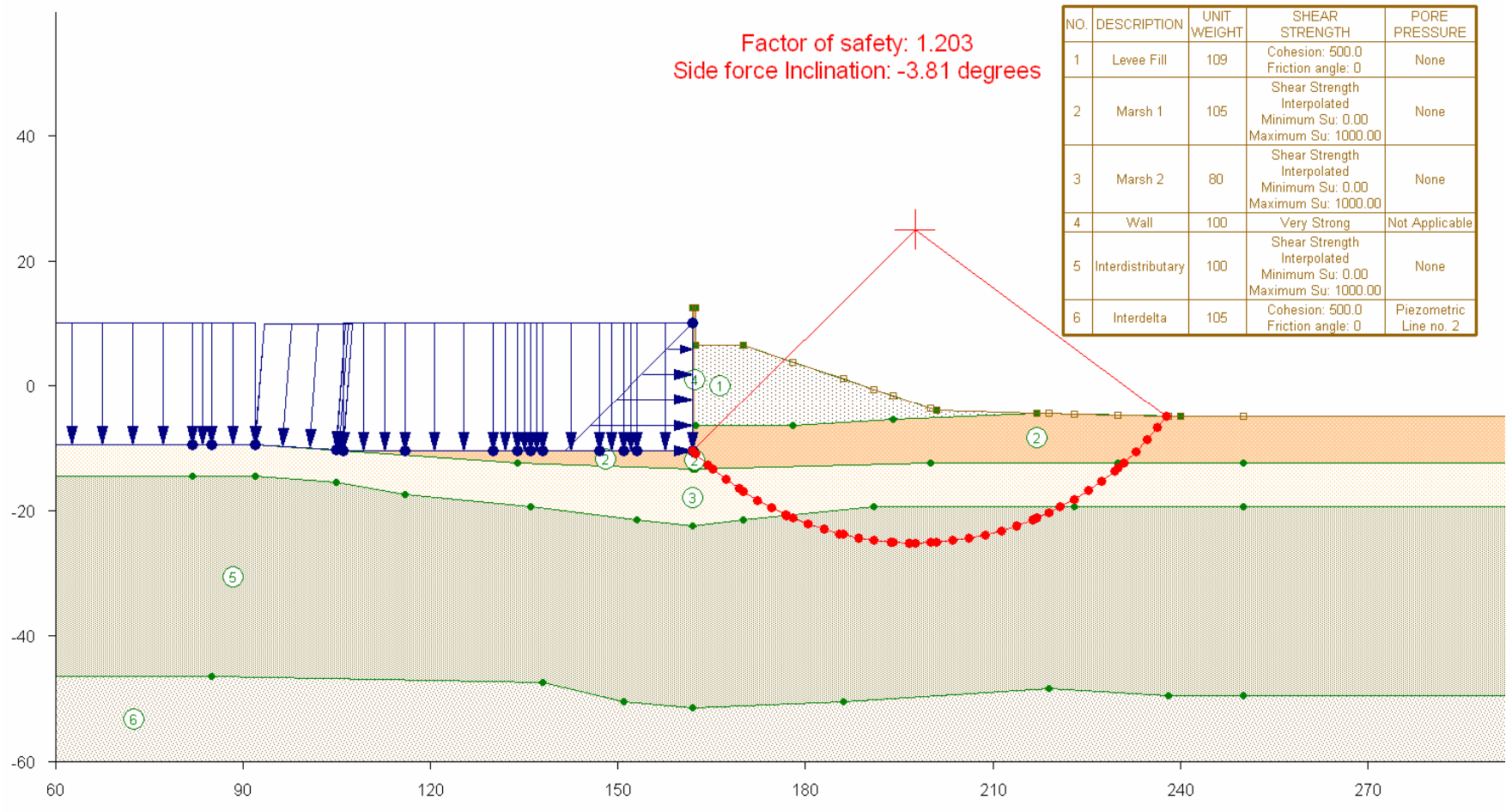


Figure 26. IHNC – East Bank (South Breach), Case 1, Canal Water Level = 10.0 ft (NAVD 88), with Crack

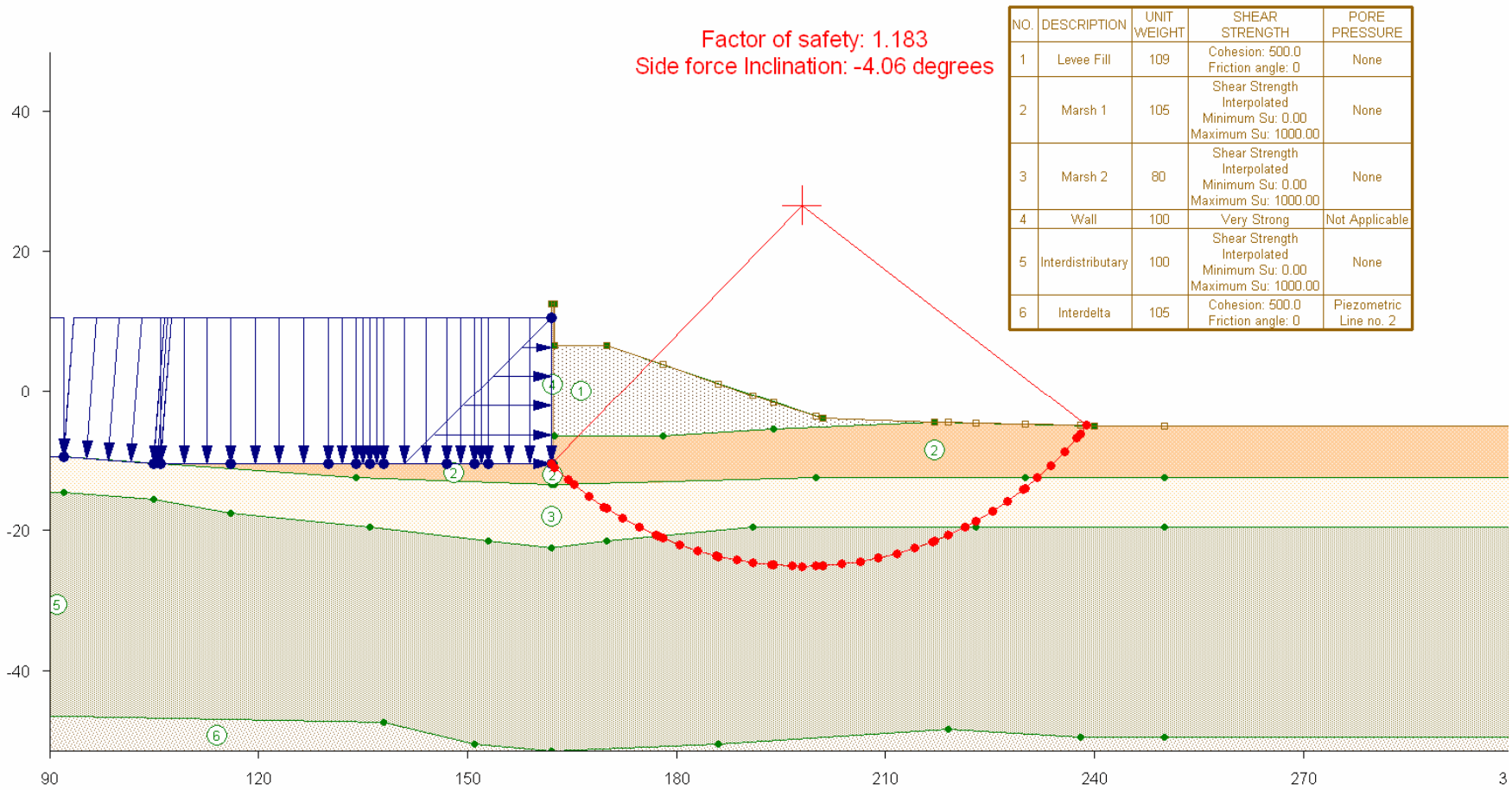


Figure 27. IHNC – East Bank (South Breach), Case 2, Design Canal Water Level = 10.5 ft (NAVD 88), with Crack

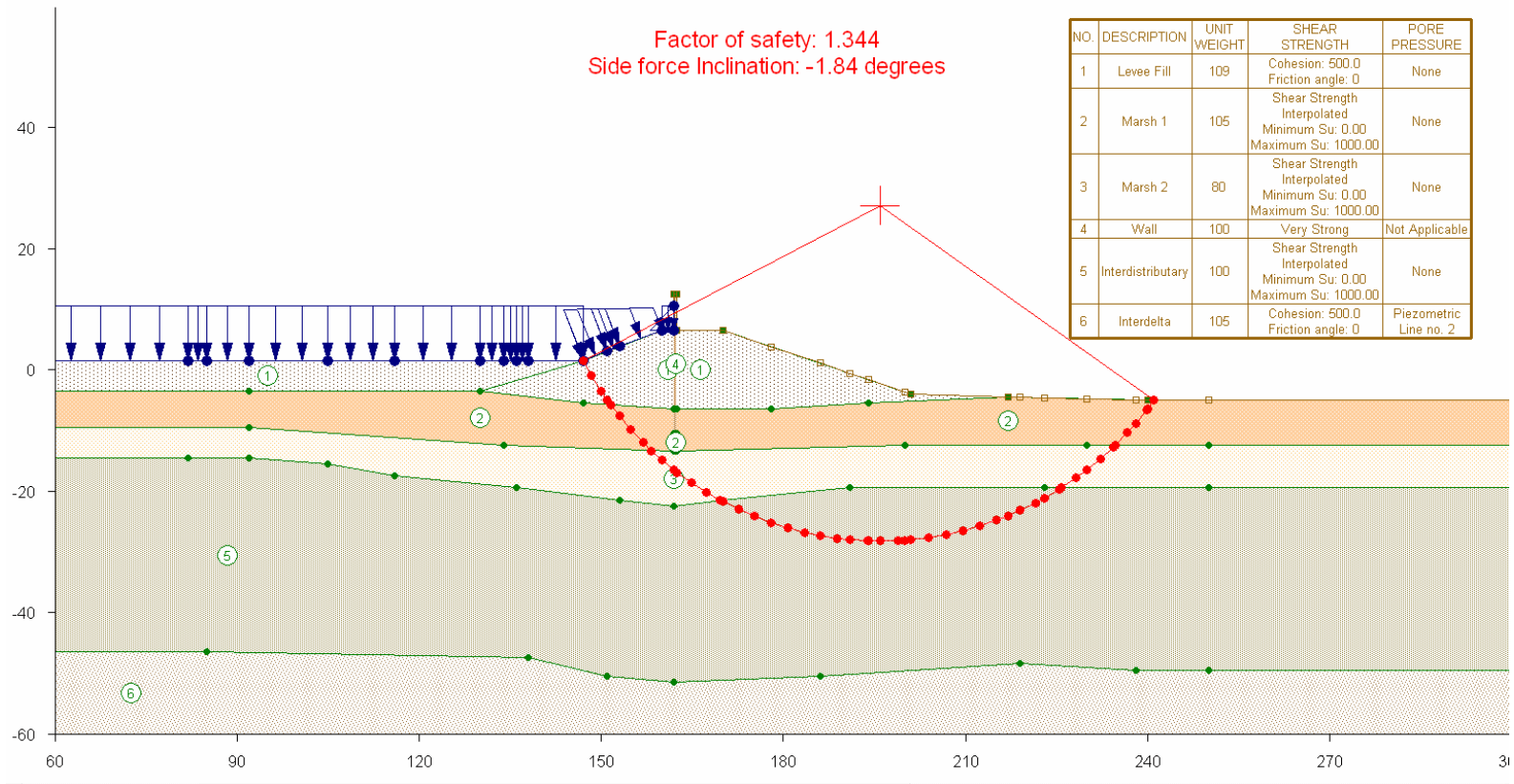


Figure 28. IHNC – East Bank (South Breach), Case 3, Design Canal Water Level = 10.5 ft (NAVD 88), without Crack

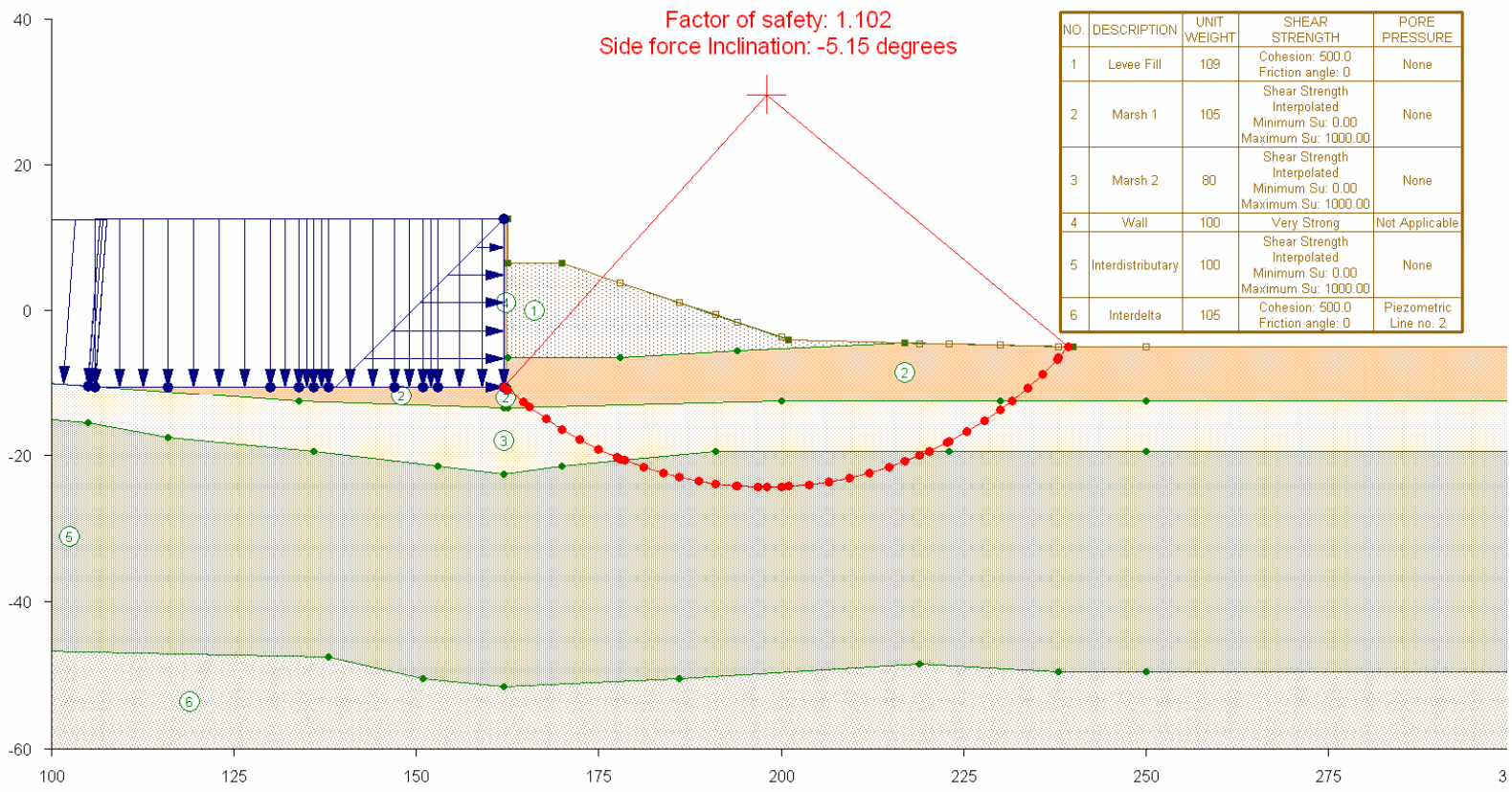


Figure 29. IHNC – East Bank (South Breach), Case 4, Canal Water Level = Top of Wall - 12.5 ft (NAVD 88), with Crack

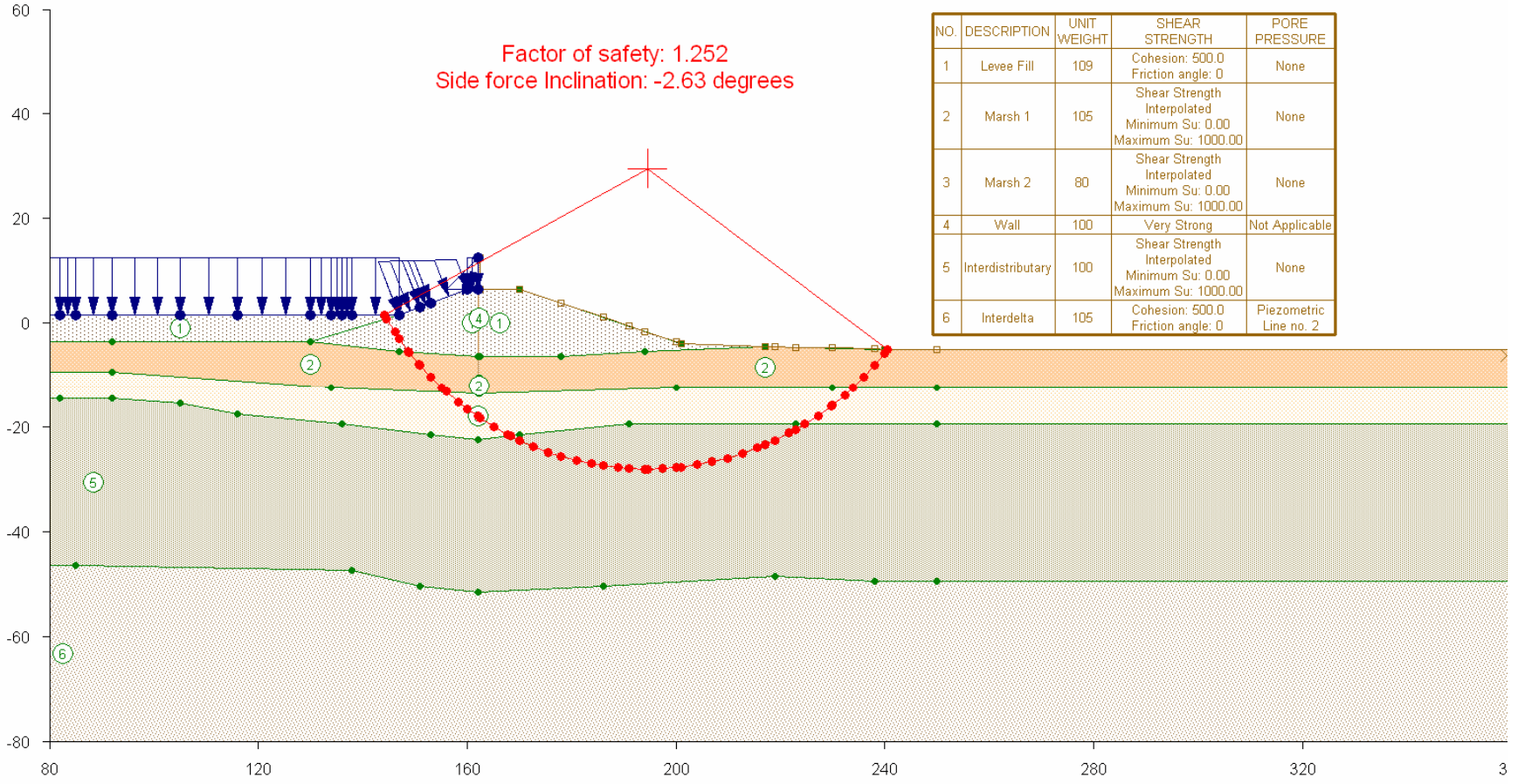


Figure 30. IHNC – East Bank (South Breach), Case 5, Canal Water Level = Top of Wall - 12.5 ft (NAVD 88), without Crack

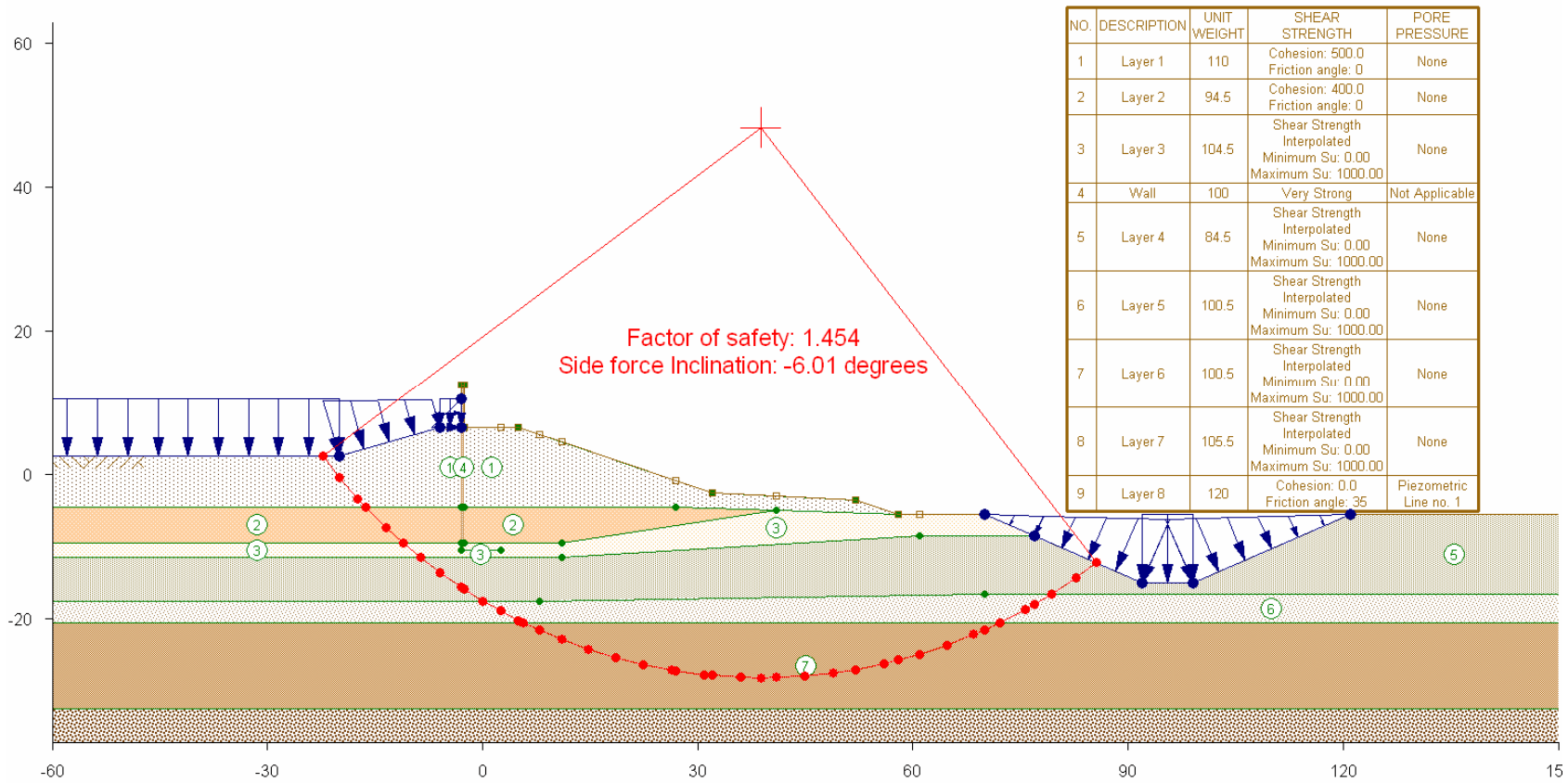


Figure 31. IHNC – East Bank (GDM Stability Plate), Case 1, Canal Water Level = Design - 10.5 ft (NAVD 88), without Crack

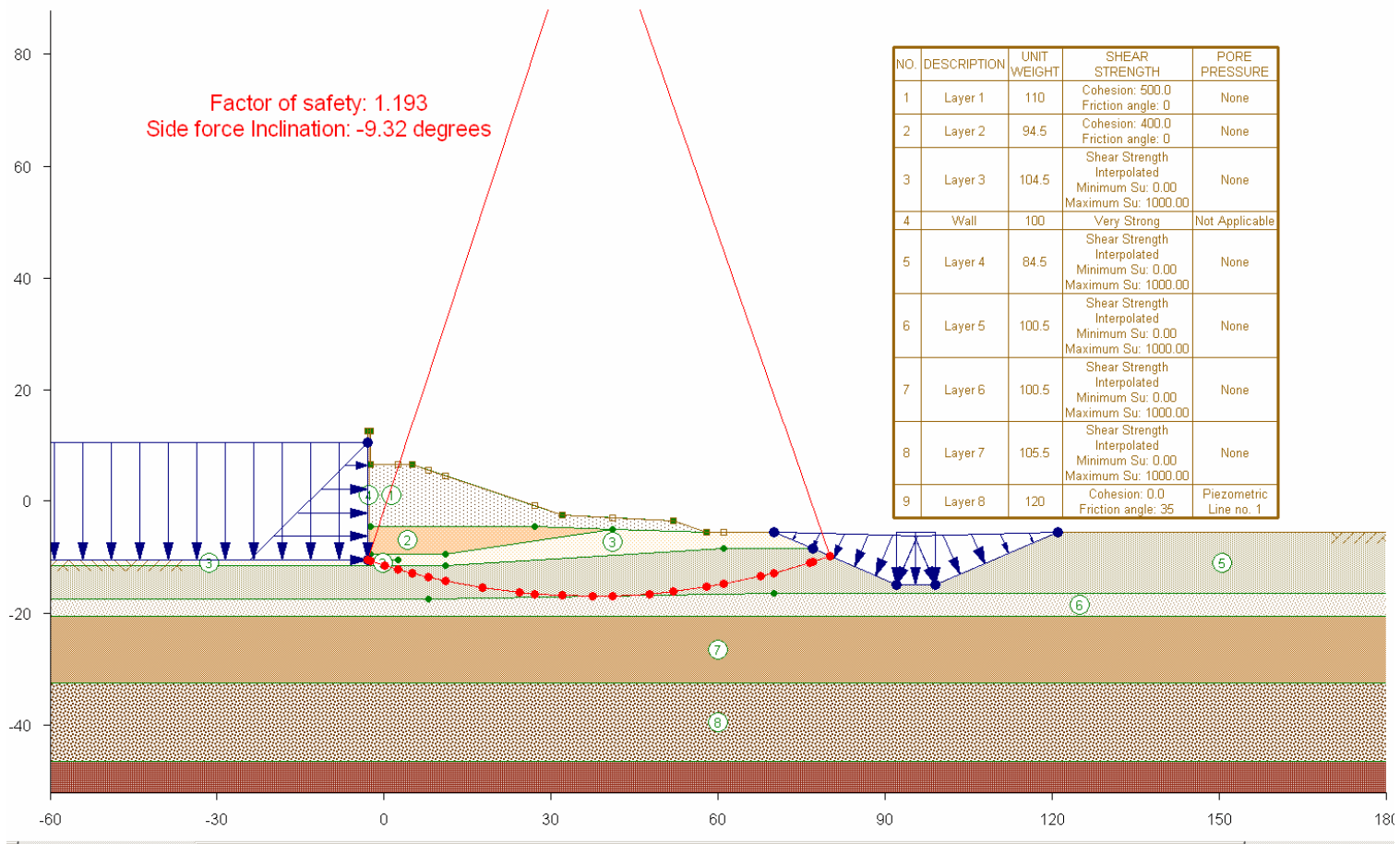


Figure 32. IHNC – East Bank (GDM Stability Plate), Case 2, Canal Water Level = Design - 10.5 ft (NAVD 88), with Crack

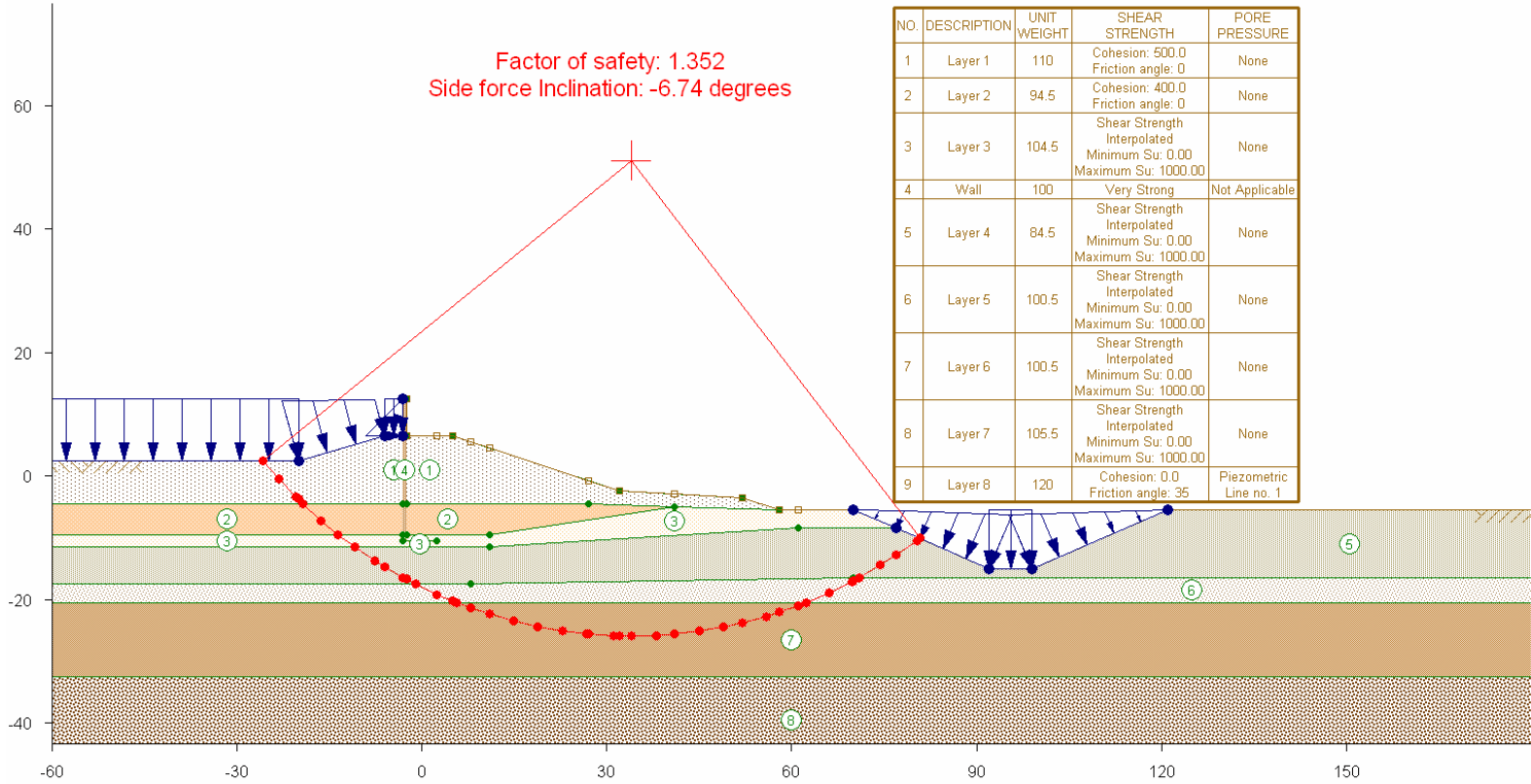


Figure 33. IHNC – East Bank (GDM Stability Plate), Case 3, Canal Water Level = Top of Wall - 12.5 ft (NAVD 88), without Crack

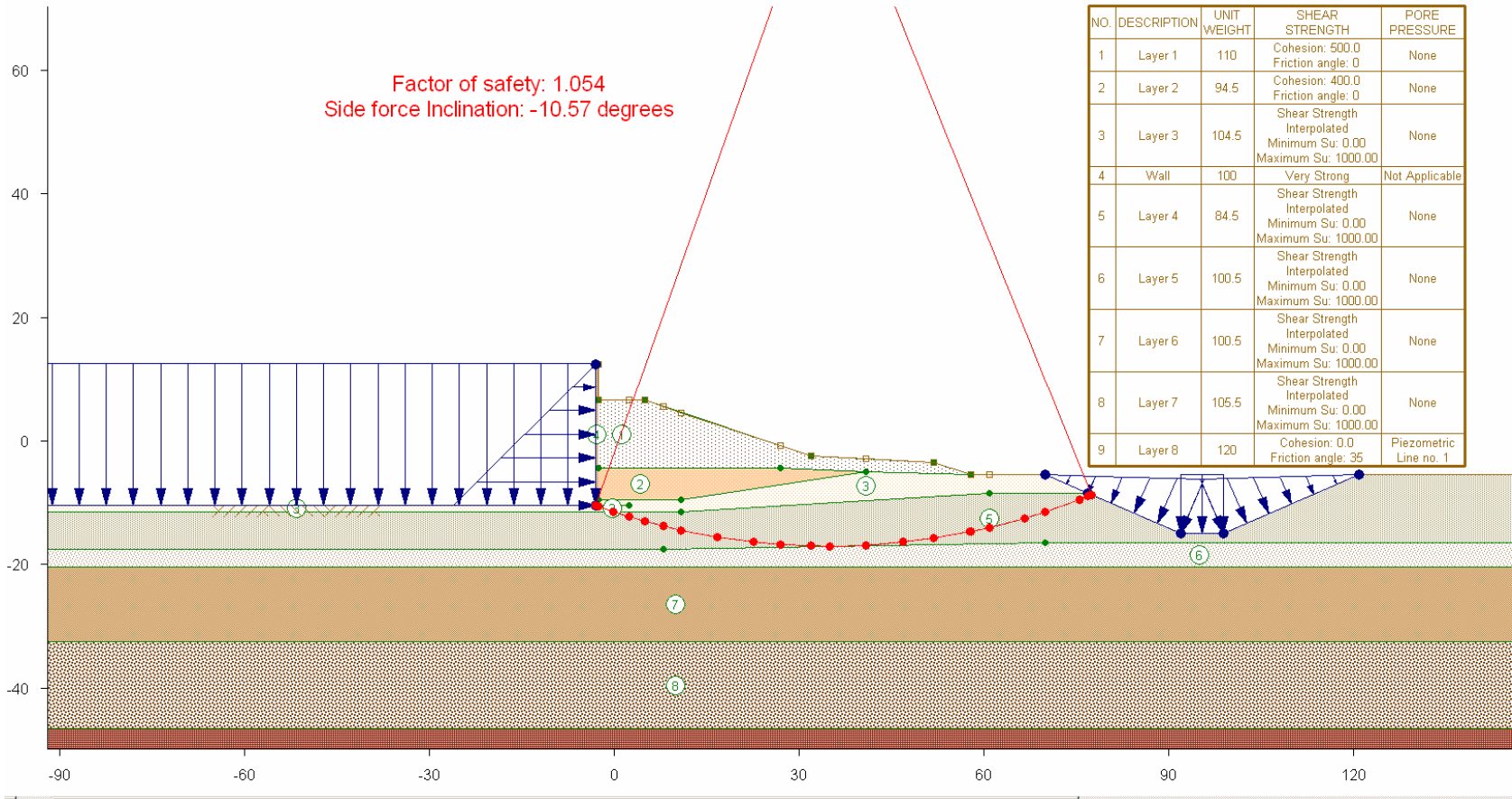


Figure 34. IHNC – East Bank (GDM Stability Plate), Case 4, Canal Water Level = Top of Wall - 12.5 ft (NAVD 88), with Crack.

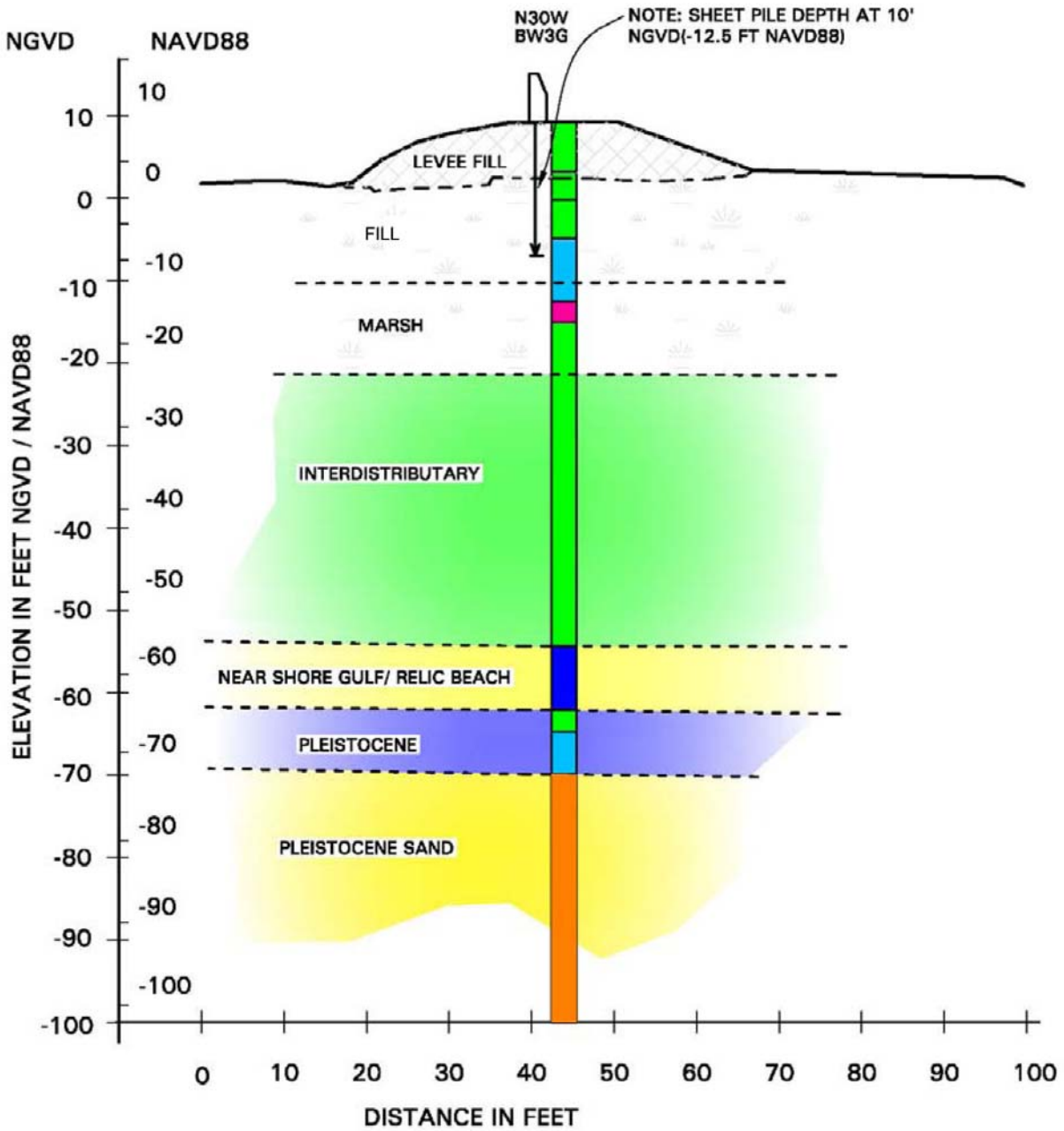


Figure 35. IHNC – West Bank – Cross section of North Breach.

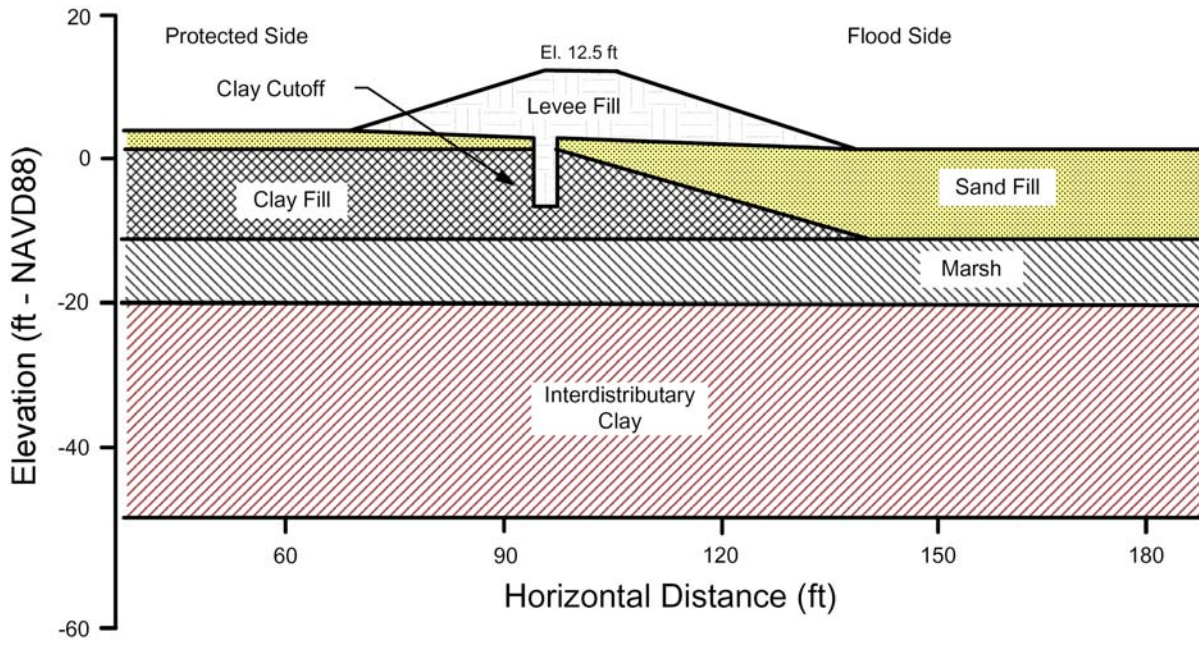


Figure 36. IHNC – West Bank – Cross section of South Breach.